

Analysis of a Sinclair-type domain decomposition solver for atomistic/continuum coupling

M. Hodapp

Skolkovo Institute of Science and Technology (Skoltech), Center for Energy Science and Technology, Moscow (RU)

Ecole polytechnique fédérale de Lausanne (EPFL), STI IGM LAMMM, Lausanne (CH)

Abstract

The “flexible boundary condition” method, introduced by Sinclair and coworkers in the 1970s, remains among the most popular methods for simulating isolated two-dimensional crystalline defects, embedded in an effectively infinite atomistic domain. In essence, the method can be characterized as a domain decomposition method which iterates between a local anharmonic and a global harmonic problem, where the latter is solved by means of the lattice Green function of the ideal crystal. This local/global splitting gives rise to tremendously improved convergence rates over related alternating Schwarz methods. In a previous publication (Hodapp et al., 2019, *Comput. Methods in Appl. Mech. Eng.* 348), we have shown that this method also applies to large-scale three-dimensional problems, possibly involving hundreds of thousands of atoms, using fast summation techniques exploiting the low-rank nature of the asymptotic lattice Green function. Here, we generalize the Sinclair method to bounded domains using a discrete boundary element method to correct the infinite solution with respect to a prescribed far-field condition, thus preserving the advantage of the original method of not requiring a global spatial discretization. Moreover, we present a detailed convergence analysis and show for a one-dimensional problem that the method is unconditionally stable under physically motivated assumptions. To further improve the convergence behavior, we develop an acceleration technique based on a relaxation of the transmission conditions between the two subproblems. Numerical examples for linear and nonlinear problems are presented to validate the proposed methodology.

Keywords: Atomistic/continuum coupling; domain decomposition; flexible boundary conditions; discrete boundary element method; convergence analysis; local/global coupling

1. Introduction

Computational physics has become a valuable tool for studying the material behavior on the nanoscale due to the vast advances in computing technology over the past 20–30 years. Presently, quantum-mechanical systems of a few hundred atoms can be simulated with density functional theory in order to predict basic material properties, such as elastic constants and phase stability. For larger systems, density functional theory becomes too expensive and problems on the nanoscale are, in lieu thereof, carried out with atomistic models.

However, atomistic models are also limited in size and time, motivating the so-called hierarchical multiscale approach in which some key parameters are calculated atomistically, such as energy barriers for defect motion, and subsequently passed to the next higher-scale level, e.g., dislocation dynamics models (see, e.g., [1]). This approach works well if the relevant mechanisms are confined to a single scale. However, there are situations where the material behavior on the smaller scale is strongly influenced by processes taking place on higher scales which requires a *concurrent multiscale approach*.

The need for concurrent multiscale models has motivated the development of atomistic/continuum (A/C) coupling methods [14, 31, 26, 27, 13]. Thereby, only the material behavior in the vicinity of crystalline defects, e.g., interstitials, vacancies, dislocations, cracks or grain boundaries, is treated fully-atomistically. This fully atomistic domain is surrounded by a significantly cheaper continuum elasticity region allowing for much larger computational domains to take scale-bridging effects into account.

A/C coupling methods can broadly be grouped into energy- and force-based methods [4]. Energy-based methods define a global energy functional which, ideally, closely reassembles the one of the fully atomistic model. However, the still existing challenge is the construction of a consistent coupling of the energy between the atomistic and continuum

E-mail address: m.hodapp@skoltech.ru

domains due to the nonlocal-local mismatch between the two models. To date, a myriad of sophisticated approaches has been developed but fully consistent methods only exist for two-dimensional problems (e.g., [21]). This motivates the use of unconditionally consistent force-based methods. In turn, however, their stability properties have not yet been fully understood [5]. Moreover, force-based methods cannot be formulated as energy minimization problems restricting the margin of possible numerical solvers.

An important task is thus to construct stable solvers for force-based A/C coupling methods. Dobson et al. [6] have proposed a monolithic Newton-GMRes method for a linearized toy model which has been shown to approximate the stability region of the fully atomistic model. Hodapp et al. [12] have extended this idea to nonlinear problems by introducing an additional criterion in order to correct the search direction whenever the atomistic Hessian becomes indefinite—which allows to overcome energy barriers, e.g., during dislocation motion. However, these methods are difficult to implement *and* parallelize in practice. A different approach is domain decomposition based on the alternating Schwarz method [33], where the coupled problem is solved sequentially by means of a fixed point iteration [22, 15]. The advantage of this method is the iteration between two *symmetric* energy minimization problems which can be solved with standard techniques. The disadvantage is, however, its poor convergence behavior which makes the method impractical as a stand-alone solver since it is potentially even slower than the fully atomistic model.

A fast alternative to the alternating Schwarz method is the “*flexible boundary condition method*” developed by Sinclair and coworkers during the 1970s [28, 29, 30]. This method can be described as a fixed point iteration between a *local anharmonic* (a.k.a. the fully atomistic) and a *global harmonic* problem. It can be shown that this splitting gives rise to significantly faster convergence rates which even compete with monolithic Krylov subspace solvers [12]. The Sinclair method has been proposed for effectively infinite problems, where the solution of the global problem reduces to a single matrix-vector multiplication exploiting the Green function of the harmonic operator, and successfully employed to study the behavior of isolated two-dimensional defects, particularly dislocations (e.g., [25, 36, 7]).

In this work, we extend the Sinclair method to bounded problems. This will be achieved by correcting the solution of the infinite problem with respect to a prescribed far-field by solving the global harmonic problem using a discrete boundary element method [18, 16, 12]. This approach is advantageous over volume-based methods, e.g., finite element methods, since boundary element methods do not require an explicit discretization of the interior of the domain which is not essential since practitioners are generally interested in the material behavior solely inside the fully atomistic domain. Moreover, the original Sinclair method is recovered if the outer boundary vanishes. Although this extension seems therefore natural, it has not yet been carried out to the best of the author’s knowledge.

Here, we focus on a one-dimensional setting which allows us to cover a detailed stability analysis of the method. It is, however, emphasized that the method itself applies generically to higher dimensions and the notation is thus kept general where possible. While numerical examples for infinite two- and three-dimensional problems have already been reported elsewhere [11, 12], a corresponding implementation for bounded problems is part of ongoing work.

The work is organized as follows. In Section 2.2 and 3, we introduce the atomistic and continuum models which are subsequently used in Section 4 to formulate the coupled problem. In Section 5, the Sinclair method for bounded problems is described and a detailed description of the proposed solution algorithm is covered. Section 6 is then devoted to the convergence analysis of the proposed algorithm. In particular, we show that the algorithm is uniformly stable under physically motivated assumptions. We also introduce a technique to further accelerate the fixed point iteration using a relaxation of the transmission conditions. This idea is extended in Section 7 to accelerate the convergence of general nonlinear problems. Numerical examples are presented in Section 8 demonstrating the efficiency of the proposed method.

2. Problem setting

We begin by formulating the reference problem. Thereby, Section 2.1 mainly serves as a brief formal introduction to set up the notation. Section 2.2 is then devoted to the definition of the atomistic model.

2.1. Notation

Computational domain. Let $\mathbb{Z}_{a_0} = a_0\mathbb{Z}$ be an infinite one-dimensional chain of atoms with lattice constant a_0 . A deformation of an atom is described via displacements $u : \mathbb{Z}_{a_0} \rightarrow \mathbb{R}$. Further, let $N \in \mathbb{N}^+$ and fix the displacement $\forall \xi < -N$ and $\forall \xi > N$ to $u(\xi) = \bar{u}(\xi)$. We thus define the space of admissible displacements as

$$\mathcal{V}(\mathbb{Z}_{a_0}) := \{ v : \mathbb{Z}_{a_0} \rightarrow \mathbb{R} \mid v(\xi) = \bar{u}(\xi) \forall \xi < -N \wedge \forall \xi > N \}. \quad (1)$$

The computational domain is then the finite subset

$$A := a_0 \{ -N, -N + 1, \dots, 0, \dots, N - 1, N \}, \quad (2)$$

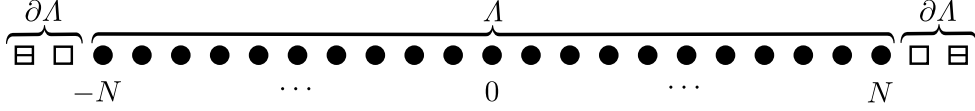


Figure 1: Atomistic domain; the highlighted atoms correspond to the following subdomains required from Section 3.2.2: $\square \rightarrow \Lambda^1$, $\boxplus \rightarrow \Lambda^1$

as shown in Figure 1, and

$$\partial\Lambda := a_0 \{ \{-O, \dots, -N-1\} \cup \{N+1, \dots, O\} \}, \quad (3)$$

its boundary, where $O > N$ depends on the interaction range of the interatomic potential (see below). In the following we denote the space of degrees of freedom by $\mathcal{V} \equiv \mathcal{V}(\Lambda)$, or $\tilde{\mathcal{V}} \equiv \mathcal{V}(\tilde{\Lambda})$ if we explicitly include the boundary displacements. In addition, we define the gradient of u in the sense of central finite differences

$$\forall \xi \in \Lambda \quad \nabla u(\xi) \equiv \frac{u(\xi + a_0) - u(\xi - a_0)}{2a_0}. \quad (4)$$

Operators. Operators acting on, e.g., \mathcal{V} , are denoted by calligraphic symbols ($\mathcal{T}, \mathcal{L}, \mathcal{G}$, etc.) and are defined as follows

$$\begin{aligned} \mathcal{T} : \mathcal{V} &\rightarrow \mathcal{V}^* \\ v &\mapsto \mathcal{T}[v] \quad \text{such that } \forall \xi \in \Lambda \quad \mathcal{T}[v](\xi) = \sum_{\eta \in \Lambda} T(\xi, \eta)v(\eta), \end{aligned} \quad (5)$$

where \mathcal{V}^* is the dual space of \mathcal{V} and $T(\xi, \eta)$ denotes the kernel of \mathcal{T} . We will often work with subspaces of \mathcal{V} . For example, let $\Lambda^1, \Lambda^2 \subset \Lambda$ such that $\Lambda^1 \cup \Lambda^2 = \Lambda$. Therefore, \mathcal{V} can be decomposed into $\mathcal{V} = \mathcal{V}(\Lambda^1) \oplus \mathcal{V}(\Lambda^2)$ and a restriction of \mathcal{T} , e.g., with respect to $\mathcal{V}(\Lambda^1)$, is denoted $\mathcal{T}^{1/1} : \mathcal{V}(\Lambda^1) \rightarrow \mathcal{V}(\Lambda^1)$. This yields the matrix representation

$$\mathcal{T} = \begin{pmatrix} \mathcal{T}^{1/1} & \mathcal{T}^{1/2} \\ \mathcal{T}^{2/1} & \mathcal{T}^{2/2} \end{pmatrix} \quad (6)$$

of which we will make frequently use of in the following. When \mathcal{T} is a linear operator, we occasionally refer to its explicit matrix representation with respect to a given basis by \underline{T} . Consequently, explicit matrix representations for vectors $v \in \mathcal{V}$ are denoted by \underline{v} . Individual elements (i, j) of \underline{T} and (i) of \underline{v} are denoted by $(\underline{T})_{i,j} = T_{i,j}$ and $(\underline{v})_i = v_i$, respectively.

Norms. For all $v \in \mathcal{V}$ we require the usual l^2 - and l^∞ -norms

$$\|v\| = \left(\sum_{\xi \in \Lambda} |v(\xi)|^2 \right)^{1/2}, \quad (7)$$

$$\|v\|_{l^\infty} = \arg \left\{ \max_{\xi \in \Lambda} v(\xi) \right\}, \quad (8)$$

as well as the inner product

$$\langle v, w \rangle = \sum_{\xi \in \Lambda} v(\xi)w(\xi), \quad \text{with } w \in \mathcal{V}. \quad (9)$$

In some cases we explicitly consider an operator \mathcal{T} as a mapping $\mathcal{T} : l^2 \rightarrow l^2$ (cf., Section 6). The corresponding operator norm, induced by l^2 , is defined as

$$\|\mathcal{T}\| = \sup_{v \neq 0} \frac{\|\mathcal{T}[v]\|}{\|v\|} = \sup_{\|v\|=1} \|\mathcal{T}[v]\| = \rho(\mathcal{T}), \quad (10)$$

where $\rho(\mathcal{T})$ is the largest singular value of \mathcal{T} .

2.2. Reference atomistic problem

Every atom $\xi \in \Lambda$ has a site energy \mathcal{E}_ξ . We assume that \mathcal{E}_ξ depends on the displacement of atom ξ relative to all other atoms within its interaction range \mathcal{R}_ξ which usually extends over a few lattice spacings (usually second- or third-nearest neighbor interactions for metals). This renders the atomistic model nonlocal, but short-range. We write this as $\{u(\eta) - u(\xi)\}_{\eta \in \mathcal{R}_\xi \setminus \xi} \equiv \{u(\eta) - u(\xi)\}$ such that $\mathcal{E}_\xi = \mathcal{E}_\xi(\{u(\eta) - u(\xi)\})$.

The total energy of the system reads

$$\Pi(u) = \Pi_0 + \Pi_{\text{int}}(u) + \Pi_{\text{ext}}(u), \quad (11)$$

where Π_0 is the energy of the ground state. For convenience we assert that $\Pi_0 = 0$ in the following. The internal and external contributions are defined as

$$\Pi_{\text{int}}(u) = \sum_{\xi \in \Lambda} \mathcal{E}_\xi(\{u(\eta) - u(\xi)\}), \quad \Pi_{\text{ext}}(u) = - \sum_{\xi \in \Lambda} f_{\text{ext}}(\xi) \cdot u(\xi), \quad (12)$$

where $f_{\text{ext}} \in \mathcal{V}^*$ is an external force. The formulation of the method does not exclude any specific type of atomic interaction per se, yet our stability analysis in Section 6.3 will be restricted to second-nearest neighbor interactions.

In this work, attention is drawn to (quasi-)static problems. That is, we seek for solutions $u \in \mathcal{V}$ which solve the optimization problem

$$u := \arg \left\{ \min_{v \in \mathcal{V}} \Pi(v) \right\}. \quad (13)$$

Solutions to (13) solve an Euler-Lagrange equation, subject to the prescribed boundary conditions on $\partial\Lambda$, i.e.,

$$\begin{cases} \mathcal{L}[u] = f_{\text{ext}} & \text{in } \Lambda, \\ u = \bar{u} & \text{on } \partial\Lambda, \end{cases} \quad (14)$$

where the nonlinear operator \mathcal{L} is defined as

$$\begin{aligned} \mathcal{L} : \bar{\mathcal{V}} &\rightarrow \mathcal{V}^* \\ v &\mapsto \mathcal{L}[v] \quad \text{such that } \forall \xi \in \Lambda \quad \mathcal{L}[v](\xi) = \delta \Pi_{\text{int}}(\xi), \end{aligned} \quad (15)$$

where $\delta \Pi_{\text{int}}(\xi)$ is the functional derivative of $\Pi_{\text{int}}(u)$ with respect to u at ξ . In the ground state, i.e., in the absence of external forces, we have $\delta \Pi_{\text{int}}(0) = 0$. In addition, we require the usual strong stability conditions on the minimizers u such that

$$\forall v \in \mathcal{V} \setminus 0 \quad \langle \delta^2 \Pi_{\text{int}}(u)[v], v \rangle > 0. \quad (16)$$

If (16) holds, it is easy to see that solutions to (14) also solve (13).

3. Continuum problem

3.1. Linearized atomistic problem

Our continuum model is based on a linearization around a uniformly deformed state $\mathbb{Z}_{a_0} + u_{\text{F}}$, where

$$\forall \xi \in \mathbb{Z}_{a_0} \quad u_{\text{F}}(\xi) = F\xi + C, \quad \text{with } F, C \geq 0. \quad (17)$$

Consider now $u = u_{\text{F}} + u'$, where u' is a perturbation of $\mathbb{Z}_{a_0} + u_{\text{F}}$. A Taylor expansion of Π to second order around u_{F} then yields the internal nonlocal harmonic energy

$$\Pi_{\text{int,hnl}}(u_{\text{F}} + u') = \frac{1}{2} \sum_{\xi \in \Lambda} \sum_{\eta \in \mathcal{R}_\xi} K_{\text{hnl}}(\xi - \eta) \cdot (u_{\text{F}}(\xi) + u'(\xi)) \cdot (u_{\text{F}}(\eta) + u'(\eta)), \quad (18)$$

where $K_{\text{hnl}}(\xi - \eta) = \delta^2 \Pi(u_{\text{F}})$ is the interatomic force constant tensor.

In addition, if the perturbation remains close to homogeneous, we can also consider a linearization of u' . That is, we apply a Taylor expansion to the displacement field and neglect higher gradients such that

$$u'(\eta) = u'(\xi) + \nabla u'(\xi)(\eta - \xi), \quad (19)$$

which is usually referred to as the Cauchy-Born hypothesis. Using (19) in (18) yields the classical definition of the internal local harmonic energy (cf., [4])

$$\Pi_{\text{int,h}}(u_{\text{F}} + u') = \frac{1}{2} \sum_{\xi \in \Lambda} \sum_{\eta \in \mathcal{R}_\xi^{\text{h}}} K_{\text{h}}(\xi - \eta) \cdot (u_{\text{F}}(\xi) + u'(\xi)) \cdot (u_{\text{F}}(\eta) + u'(\eta)), \quad (20)$$

where $K_h(\xi - \eta)$ is the local version of $K_{\text{hnl}}(\xi - \eta)$ and \mathcal{R}_ξ^h is the interaction range of the local harmonic site energy which comprises first nearest neighbors. We define

$$K_h(\xi - \eta) = \begin{cases} -\bar{k} & \text{if } |\xi - \eta| = a_0, \\ 2\bar{k} & \text{if } |\xi - \eta| = 0, \\ 0 & \text{else,} \end{cases} \quad (21)$$

and assume that $\bar{k} > 0$ in the following. The Euler-Lagrange equation of the local harmonic problem then reads

$$\mathcal{L}_h[u](\xi) = -\bar{k}(u(\xi - a_0) - 2u(\xi) + u(\xi + a_0)) = f_{\text{ext}}(\xi) \quad \forall \xi \in \Lambda. \quad (22)$$

3.2. Discrete boundary element method

Boundary element methods for lattice problems have been proposed by Martinsson [18] for the discrete Laplace equation and in the context of atomistic/continuum coupling by Li [16] and Hodapp et al. [12]. By using a *discrete boundary element method*, we do not have to resort back to a “true” continuum model and can consider arbitrary interaction stencils, i.e., all subsequent developments generically apply to local and nonlocal elasticity models (cf., Section 3.1). Moreover, it is worthwhile noting that fast summation techniques, such as the fast multipole method [9] or hierarchical matrices [34, 10], readily apply to the discrete case as demonstrated in [19, 12].

In the following we briefly summarize the basic ideas following the notation from [12].

3.2.1. Lattice Green function

Consider the infinite harmonic problem, subject to a unit point force

$$\mathcal{L}_h[u] = \delta \quad \text{in } \mathbb{Z}_{a_0}, \quad \text{where } \forall \xi \in \mathbb{Z}_{a_0} \quad \delta(\xi) = \begin{cases} 1 & \text{if } \xi = 0, \\ 0 & \text{else.} \end{cases} \quad (23)$$

The Green operator is defined as

$$\begin{aligned} \mathcal{G} : \mathcal{V}^*(\mathbb{Z}_{a_0}) &\rightarrow \mathcal{V}(\mathbb{Z}_{a_0}) \\ \delta &\mapsto \mathcal{G}[\delta] \quad \text{such that } \forall \xi \in \mathbb{Z}_{a_0} \quad \mathcal{G}[\delta](\xi) = \sum_{\eta \in \mathbb{Z}_{a_0}} G(\xi - \eta)\delta(\eta) = u(\xi), \end{aligned} \quad (24)$$

where $G(\xi - \eta)$ is the lattice Green function. This implies the identity relation

$$(\mathcal{G}\mathcal{L}_h)[u] = \mathcal{I}[u] \quad \text{in } \mathbb{Z}_{a_0}, \quad \text{where} \quad \mathcal{I}[u](\xi) = \sum_{\eta \in \mathbb{Z}_{a_0}} \delta(\xi - \eta)u(\eta) = u(\xi) \quad (25)$$

of which we shall make frequently use of in the following (here, \mathcal{I} denotes the identity operator).

The Green function corresponding to \mathcal{L}_h reads

$$G(\xi - \eta) = -\frac{1}{2\bar{k}a_0}|\xi - \eta| + C, \quad \text{with } C \in \mathbb{R}, \quad (26)$$

which can be obtained by means of semi-discrete Fourier transforms (e.g., [32]). The choice of the constant C is, in principle, arbitrary since the mapping (23) is not bijective but there are particular useful choices which render the linear system associated with the harmonic problem positive definite (see Remark 1 in Section 3.2.3).

3.2.2. Boundary summation equation

It is possible to write the solution of (22) solely in terms of the degrees of freedom on the boundary $\partial\Lambda \equiv \Lambda^I$. This procedure can be considered as the analog to the “integration by parts” in continuum mechanics leading to a boundary summation equation, a discrete variant of the boundary integral equation.

First, we extend the domain of \mathcal{L}_h to $\bar{\mathcal{V}}$ and presume that $f_{\text{ext}} = 0$. That is, we consider

$$\mathcal{L}_h[u] = 0 \quad \text{in } \bar{\Lambda}. \quad (27)$$

Next, we split $\mathcal{L}_h[u]$ as follows

$$\mathcal{L}_h[u] = \mathcal{L}_h^{\bar{\Lambda}/\bar{\Lambda} \cup I^-}[u] = \mathcal{L}_h^{\bar{\Lambda}/\bar{\Lambda}}[u] + \mathcal{L}_h^{\bar{\Lambda}/I^-}[u], \quad (28)$$

where the superscripted domains and codomains on the right hand side refer to the function spaces on the sets defined in Figure 1. We now apply $\mathcal{G}^{\bar{\Lambda}/\bar{\Lambda}}$ to (28) which yields

$$(\mathcal{G}^{\bar{\Lambda}/\bar{\Lambda}}\mathcal{L}_h^{\bar{\Lambda}/\bar{\Lambda}\cup I^-})[u] = (\mathcal{G}^{\bar{\Lambda}/\bar{\Lambda}}\mathcal{L}_h^{\bar{\Lambda}/\bar{\Lambda}})[u] + (\mathcal{G}^{\bar{\Lambda}/\bar{\Lambda}}\mathcal{L}_h^{\bar{\Lambda}/I^-})[u]. \quad (29)$$

The idea is now to rewrite (29) in a way that reveals the sparsity of $\mathcal{G}^{\bar{\Lambda}/\bar{\Lambda}}\mathcal{L}_h^{\bar{\Lambda}/\bar{\Lambda}}$. For this purpose, we decompose the domain and co-domain of $\mathcal{G}\mathcal{L}_h$ (eq. (25)) into $\bar{\Lambda}$ and the infinite remainder $\Lambda^r = \mathbb{Z}_{a_0} \setminus \bar{\Lambda}$, i.e.,

$$\begin{aligned} \mathcal{G}\mathcal{L}_h &= \begin{pmatrix} \mathcal{G}^{\bar{\Lambda}/\bar{\Lambda}} & \mathcal{G}^{\bar{\Lambda}/r} \\ \mathcal{G}^{r/\bar{\Lambda}} & \mathcal{G}^{r/r} \end{pmatrix} \begin{pmatrix} \mathcal{L}_h^{\bar{\Lambda}/\bar{\Lambda}} & \mathcal{L}_h^{\bar{\Lambda}/r} \\ \mathcal{L}_h^{r/\bar{\Lambda}} & \mathcal{L}_h^{r/r} \end{pmatrix} \\ &= \begin{pmatrix} \mathcal{G}^{\bar{\Lambda}/\bar{\Lambda}}\mathcal{L}_h^{\bar{\Lambda}/\bar{\Lambda}} + \mathcal{G}^{\bar{\Lambda}/r}\mathcal{L}_h^{r/\bar{\Lambda}} & \mathcal{G}^{r/r}\mathcal{L}_h^{r/\bar{\Lambda}} + \mathcal{G}^{\bar{\Lambda}/\bar{\Lambda}}\mathcal{L}_h^{\bar{\Lambda}/\bar{\Lambda}} \\ \mathcal{G}^{\bar{\Lambda}/r}\mathcal{L}_h^{r/r} + \mathcal{G}^{\bar{\Lambda}/\bar{\Lambda}}\mathcal{L}_h^{\bar{\Lambda}/r} & \mathcal{G}^{\bar{\Lambda}/r}\mathcal{L}_h^{r/\bar{\Lambda}} + \mathcal{G}^{\bar{\Lambda}/\bar{\Lambda}}\mathcal{L}_h^{\bar{\Lambda}/\bar{\Lambda}} \end{pmatrix} = \begin{pmatrix} \mathcal{I}^{\bar{\Lambda}/\bar{\Lambda}} & \mathbf{0}^{\bar{\Lambda}/r} \\ \mathbf{0}^{r/\bar{\Lambda}} & \mathcal{I}^{r/r} \end{pmatrix}. \end{aligned} \quad (30)$$

In addition, we recall that the coupling operators $\mathcal{L}_h^{\bar{\Lambda}/r}$ and $\mathcal{L}_h^{r/\bar{\Lambda}}$ satisfy the following relations $\forall v$

$$\mathcal{L}_h^{\bar{\Lambda}/r}[v] = 0 \quad \text{in } \Lambda^{\bar{\Lambda}} \setminus \Lambda^I, \quad \mathcal{L}_h^{\bar{\Lambda}/r \setminus I^-}[v] = 0 \quad \text{in } \Lambda^I, \quad (31)$$

$$\mathcal{L}_h^{r/\bar{\Lambda}}[v] = 0 \quad \text{in } \Lambda^r \setminus \Lambda^{I^-}, \quad \mathcal{L}_h^{r/\bar{\Lambda} \setminus I}[v] = 0 \quad \text{in } \Lambda^{I^-}, \quad (32)$$

which follow from the definition of \mathcal{L}_h . With (30) and (31), $(\mathcal{G}^{\bar{\Lambda}/\bar{\Lambda}}\mathcal{L}_h^{\bar{\Lambda}/\bar{\Lambda}})[u]$ from (29) can now be rewritten as

$$(\mathcal{G}^{\bar{\Lambda}/\bar{\Lambda}}\mathcal{L}_h^{\bar{\Lambda}/\bar{\Lambda}})[u] = \mathcal{I}^{\bar{\Lambda}/\bar{\Lambda}}[u] - (\mathcal{G}^{\bar{\Lambda}/r}\mathcal{L}_h^{r/\bar{\Lambda}})[u] = \mathcal{I}^{\bar{\Lambda}/\bar{\Lambda}}[u] - (\mathcal{G}^{\bar{\Lambda}/I^-}\mathcal{L}_h^{I^-/I})[u]. \quad (33)$$

Vice versa, with (32), we can write $(\mathcal{G}^{\bar{\Lambda}/\bar{\Lambda}}\mathcal{L}_h^{\bar{\Lambda}/I^-})[u]$ from (29) as

$$(\mathcal{G}^{\bar{\Lambda}/\bar{\Lambda}}\mathcal{L}_h^{\bar{\Lambda}/I^-})[u] = (\mathcal{G}^{\bar{\Lambda}/I}\mathcal{L}_h^{I/I^-})[u]. \quad (34)$$

Using (33) and (34) in (29) and re-arranging some of the terms, we obtain the *boundary summation equation* which yields the following expression for the displacements (cf., [12])

$$u = \mathcal{F}^{\bar{\Lambda}/I}[u] - \mathcal{G}^{\bar{\Lambda}/I}[f] \quad \text{in } \bar{\Lambda}, \quad (35)$$

with $\mathcal{F}^{\bar{\Lambda}/I} = \mathcal{G}^{\bar{\Lambda}/I^-}\mathcal{L}_h^{I^-/I}$ and $f^I = \mathcal{L}_h^{I/I^-}[u]$.

3.2.3. Solution procedure

Equation (35) can now be used to solve the general inhomogeneous problem (22). Therefore, we split (22) into two parts: an inhomogeneous infinite problem (\tilde{P}) and a finite homogeneous problem (\hat{P}) which corrects (\tilde{P}) to account for the prescribed boundary condition on Λ^I . That is, we seek for \tilde{u} and \hat{u} such that

$$(\tilde{P}) \quad \mathcal{L}_h[\tilde{u}] = f_{\text{ext}} \quad \text{in } \mathbb{Z}_{a_0}, \quad (\hat{P}) \quad \begin{cases} \mathcal{L}_h[\hat{u}] = 0 & \text{in } \Lambda^c, \\ \hat{u} = \bar{u} - \tilde{u} & \text{on } \Lambda^I. \end{cases} \quad (36)$$

The full solution is then given $\forall \xi \in \Lambda$ as $u(\xi) = \tilde{u}(\xi) + \hat{u}(\xi)$. Algorithm 1 summarizes this solution procedure.

Algorithm 1: Discrete boundary element method (DBEM)

Input: boundary condition \bar{u}^I , external force f_{ext}

- 1 $\tilde{u}^{\bar{\Lambda}} \leftarrow \mathcal{G}^{\bar{\Lambda}/\Lambda}[f_{\text{ext}}]$; // solve (\tilde{P})
- 2 $w \leftarrow (\mathcal{I}^{I/I} - \mathcal{F}^{I/I})[\bar{u} - \tilde{u}]$; // compute right hand side of the linear system
- 3 $f^I \leftarrow -\mathcal{G}^{I/I^-}[w]$; // solve linear system for the boundary forces f^I
- 4 $\hat{u}^{\Lambda} \leftarrow \mathcal{F}^{\Lambda/I}[\bar{u} - \tilde{u}] - \mathcal{G}^{\Lambda/I}[f]$; // compute solution of (\hat{P})
- 5 $u^{\Lambda} \leftarrow \tilde{u}^{\Lambda} + \hat{u}^{\Lambda}$; // assemble full solution

Output: solution u^{Λ}

It is emphasized that the evaluation of the solution in the entire domain is usually prohibitive for three dimensional problems—even with fast summation techniques, such as fast multipole methods or hierarchical matrices (\mathcal{H} -matrices). Fortunately, in the particular case of atomistic/continuum coupling, the solution is only required in the vicinity of the artificial interface as will be discussed in the following section. This makes boundary element methods particularly efficient for this class of problems.

Remark 1. *The linear system in line 3 of Algorithm 1 is, unlike in the case of finite element methods, not necessarily positive definite due to non-uniqueness of \mathcal{G} . This can be deduced from the eigenvalues of*

$$\underline{\underline{G}}^{I/I} \equiv \begin{pmatrix} G(0) & G(-2N) \\ G(-2N) & G(0) \end{pmatrix} = \begin{pmatrix} C & -\frac{N}{ka_0} \\ -\frac{N}{ka_0} & C \end{pmatrix} \quad (37)$$

which are given by $C + \bar{k}/a_0$ and $C - \bar{k}/a_0$. It can now be easily seen that $\underline{\underline{G}}^{I/I}$ can be made positive definite if $C > \bar{k}/a_0$, indefinite if $-\bar{k}/a_0 < C < \bar{k}/a_0$ or negative definite if $C < -\bar{k}/a_0$.

Similar arguments also apply in two and three dimensions which permits the use of the conjugate gradient method. However, it should be noted that the minimal residual method will be unconditionally stable.

Remark 2 (Treatment of the outer boundary). *For large computational domains, especially in three dimensions, the outer boundary contains substantially more degrees of freedom than the inner boundary. Therefore, even with fast summation techniques, it might be beneficial to seek for solutions in a subspace of $\mathcal{V}(\Lambda^I)$. A first step in that direction has been taken by Li [16] who proposed a $\mathbb{P}1$ interpolation of u over a reduced set of nodes on Λ^I .*

4. Force-based coupled atomistic/continuum problem

In this section the atomistic/continuum (A/C) coupling scheme is described. First, we define the fully atomistic domain as a subset of Λ

$$\Lambda^a := a_0 \{ -M, -M + 1, \dots, 0, \dots, M - 1, M \}, \quad (38)$$

with $M \ll N$, in general. The atomistic domain is then surrounded by the continuum region

$$\Lambda^c := a_0 \{ -N, \dots, -M - 1 \} \cup \{ M + 1, \dots, N \} \quad (39)$$

such that $\Lambda := \Lambda^a \cup \Lambda^c$, as shown in Figure 2.

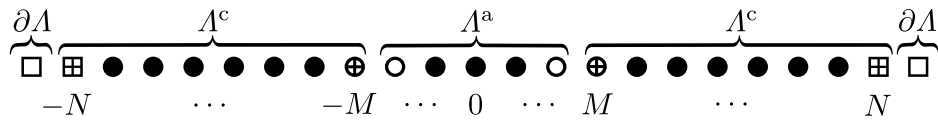


Figure 2: Computational domain divided into an atomistic and a continuum domain; the highlighted subdomains are defined as follows: $\circ \rightarrow \Lambda^i$, $\oplus \rightarrow \Lambda^{i+}$, $\square \rightarrow \Lambda^I$ and $\boxplus \rightarrow \Lambda^{I+}$

We restrict nonlinear material behavior occurring in the neighborhood of lattice defects, e.g., vacancies, interstitials or dislocations (only in two and three dimensions, respectively), to the atomistic domain. The continuum domain is assumed to be defect-free. Hence:

Assumption 1 (Linear elasticity). *The material behavior in Λ^c is adequately represented by the linear elastic energy functional (20).*

At the artificial boundary between the two domains, atoms in Λ^a can interact with continuum nodes in $\Lambda^p \subset \Lambda^c$ according to their interaction law, where Λ^p is referred to as the pad region. Vice versa, according to Assumption 1, continuum nodes in Λ^{i+} interact with the interface atoms in Λ^i , while the outer interface $\Lambda^I \equiv \partial\Lambda$ provides the natural boundary conditions.

The coupled problem is then defined as follows: find $u \in \mathcal{V}$ such that

$$(P^a) \begin{cases} \mathcal{L}[\{u^a, u^p\}] = f_{\text{ext}} & \text{in } \Lambda^a, \\ u = u^c & \text{in } \Lambda^p, \end{cases} \quad (P^c) \begin{cases} \mathcal{L}_h[\{u^c, u^i, u^I\}] = f_{\text{ext}} & \text{in } \Lambda^a, \\ u = u^a & \text{on } \Lambda^i, \\ u = \bar{u} & \text{on } \Lambda^I. \end{cases} \quad (40)$$

The distinct advantage of force-based methods is the consistency of the coupling, i.e., no spurious forces arise in the vicinity of the artificial interface due to the nonlocal-local mismatch between the two models. Their disadvantage is, however, the lack of a well-defined energy functional. This restricts the choice of possible monolithic solvers to multidimensional root-finding methods, e.g., the generalized minimal residual method [6].

Therefore, another popular choice are domain decomposition solvers based on the alternating Schwarz method which iteratively solve two energy minimization problems in Λ^a and Λ^c , bypassing the concurrent coupling (e.g., [22, 16, 23]). However, they usually converge very slowly (potentially even slower than a model with fully atomistic resolution), even with sophisticated acceleration techniques, such as overlapping subdomains, which makes A/C coupling counterproductive. The aim of this work is thus to develop a new domain decomposition solver with improved convergence behavior over these existing methods.

5. Sinclair method for bounded problems

In the 1970s, Sinclair and coworkers introduced a fast alternative to the alternating Schwarz method to solve atomistic problems which are embedded in an effectively infinite domain. In [12], we have shown that the excellent convergence properties of the Sinclair method are due to the particular splitting of the coupled operator into a finite anharmonic and a global infinite harmonic part. This splitting procedure is analog for bounded problems as will be demonstrated below.

Definition 1 (Anharmonic/harmonic operator split). Let \mathcal{L}_{cpl} be the differential operator associated with the coupled problem (40). We then denote the anharmonic/harmonic operator split as the additive decompositions

$$\mathcal{L}_{\text{cpl}} = \mathcal{L}_{\text{ah}} + \mathcal{L}_{\text{h}}, \quad u = u_{\text{ah}} + u_{\text{h}} \quad (41)$$

into anharmonic parts $\mathcal{L}_{\text{ah}}, u_{\text{ah}}$, and harmonic parts $\mathcal{L}_{\text{h}}, u_{\text{h}}$, with

$$\mathcal{L}_{\text{ah}} = \begin{pmatrix} \mathcal{L}_{\text{ah}}^{a/\bar{\Lambda}} - \mathcal{L}_{\text{h}}^{a/\bar{\Lambda}} \\ \mathbf{0}^{c/\bar{\Lambda}} \end{pmatrix}, \quad u_{\text{ah}}^{\bar{c}} = 0, \quad (42)$$

where the superscripted index \bar{c} refers to the domain $\Lambda^c \cup \Lambda^I$.

Using (41) from Definition 1 and exploiting the linearity of the harmonic operator we can write the coupled problem (40) as follows

$$\mathcal{L}_{\text{cpl}}[u] = \mathcal{L}_{\text{ah}}[u] + \mathcal{L}_{\text{h}}[u_{\text{ah}}] + \mathcal{L}_{\text{h}}[u_{\text{h}}] = f_{\text{ext}} \quad \text{in } \Lambda, \quad (43)$$

omitting the natural boundary conditions. Now we set $u_{\text{ah}}^{\bar{c}} = 0$ and re-arrange (40) as follows

$$\mathcal{L}_{\text{cpl}}[u] - \mathcal{L}_{\text{h}}[u] + \mathcal{L}_{\text{h}}[u_{\text{h}}] + \mathcal{L}_{\text{h}}^{a/a}[u_{\text{ah}}] = f_{\text{ext}} \quad \text{in } \Lambda, \quad (44)$$

where $\mathcal{L}_{\text{cpl}}[u] - \mathcal{L}_{\text{h}}[u] = \mathcal{L}_{\text{ah}}[u]$. Putting f_{ext} on the left hand side of the equation, we obtain

$$\underbrace{\begin{pmatrix} \mathcal{L}^a[u] \\ 0 \end{pmatrix} - \begin{pmatrix} f_{\text{ext}}^a \\ 0 \end{pmatrix}}_{\text{(AH)}} + \underbrace{\begin{pmatrix} \mathcal{L}_{\text{h}}^{a/a} & \mathcal{L}_{\text{h}}^{a/\bar{c}} \\ \mathcal{L}_{\text{h}}^{c/a} & \mathcal{L}_{\text{h}}^{c/\bar{c}} \end{pmatrix} \begin{bmatrix} u_{\text{h}}^a \\ u_{\text{h}}^{\bar{c}} \end{bmatrix} - \begin{pmatrix} \mathcal{L}_{\text{h}}^{a/a}[u_{\text{h}}] + \mathcal{L}_{\text{h}}^{a/\bar{c}}[u] \\ -\mathcal{L}_{\text{h}}^{c/a}[u_{\text{ah}}] + f_{\text{ext}}^c \end{pmatrix}}_{\text{(H)}} = \begin{pmatrix} 0 \\ 0 \end{pmatrix} \quad \text{in } \Lambda, \quad (45)$$

where the anharmonic problem **(AH)** and the harmonic problem **(H)** are coupled through the solution in Λ^P and Λ^I , respectively.

To solve (45), a staggered procedure is proposed which iterates between **(AH)** and **(H)**. Therefore, let us denote $k \in \mathbb{N}$ as the global iteration index and fix an initial guess u_0 . The $k+1$ -th iteration then reads

$$\text{(AH)}_{k+1} \begin{cases} \mathcal{L}[\{u_{k+1}^a, u_{k+1}^P\}] = f_{\text{ext}} & \text{in } \Lambda^a, \\ u_{k+1} = u_k^c & \text{in } \Lambda^P, \end{cases} \quad \text{(H)}_{k+1} \begin{cases} \mathcal{L}_{\text{h}}[u_{\text{h},k+1}] = \mathcal{L}_{\text{h}}^{a/a}[u_{\text{h},0}] + \mathcal{L}_{\text{h}}^{a/\bar{c}}[u_0] & \text{in } \Lambda^a, \\ \mathcal{L}_{\text{h}}[u_{\text{h},k+1}] = -\mathcal{L}_{\text{h}}^{c/a}[u_{\text{ah},k+1}] + f_{\text{ext}} & \text{in } \Lambda^c, \\ u = \bar{u} & \text{on } \Lambda^I. \end{cases} \quad (46)$$

Note that **(AH)** is a finite problem, defined in Λ^a and **(H)** is a global problem, defined in the entire domain $\Lambda := \Lambda^a \cup \Lambda^c$.

At first glance, it seems natural to choose the global harmonic solution as an initial guess. However, there are situations where linear elasticity is a bad approximation of the coupled problem (cf., Section 8.2). Fortunately, in

such cases we can initialize the algorithm with $u_0 = 0$ without actually influencing the convergence rate. This will be demonstrated, i.a., in the following section.

Furthermore, one would like to avoid to work with the source term $\mathcal{L}_h^{c/a}[u_{\text{ah},k+1}]$ of $(\mathbf{H})_{k+1}$ in practice, taking into account that $u_{\text{h},k+1}^a$ needs to be evaluated in the *entire* atomistic domain to compute $u_{\text{ah},k+1}^a = u_{k+1}^a - u_{\text{h},k+1}^a$ explicitly. Fortunately, it is possible to solve $(\mathbf{H})_{k+1}$ using solely the total solution u . To see this, consider the solution to the harmonic problem in step $k+1$

$$\begin{pmatrix} u_{\text{h},k+1}^a \\ u_{k+1}^c \end{pmatrix} = \begin{pmatrix} \mathcal{L}_h^{a/a} & \mathcal{L}_h^{a/c} \\ \mathcal{L}_h^{c/a} & \mathcal{L}_h^{c/c} \end{pmatrix}^{-1} \begin{bmatrix} f_{\text{ext}}^a \\ -\mathcal{L}_h^{c/a}[u_{\text{ah},k+1}] - \mathcal{L}_h^{c/I}[u] + f_{\text{ext}}^c \end{bmatrix}. \quad (47)$$

By subtracting $u_{\text{h},k}$ from $u_{\text{h},k+1}$ we obtain

$$\begin{pmatrix} u_{\text{h},k+1}^a \\ u_{k+1}^c \end{pmatrix} = \begin{pmatrix} u_{\text{h},k}^a \\ u_k^c \end{pmatrix} - \begin{pmatrix} \mathcal{L}_h^{a/a} & \mathcal{L}_h^{a/c} \\ \mathcal{L}_h^{c/a} & \mathcal{L}_h^{c/c} \end{pmatrix}^{-1} \begin{bmatrix} 0 \\ \mathcal{L}_h^{c/a}[\Delta u_{\text{ah},k}] \end{bmatrix}, \quad (48)$$

where $\Delta u_{\text{ah},k} = u_{\text{ah},k+1} - u_{\text{ah},k}$. To obtain an expression of $\mathcal{L}_h^{c/a}[\Delta u_{\text{ah},k}]$ in terms of the full solution u only, consider

$$\mathcal{L}_h^{c/a}[u_{\text{ah},k}] = -\mathcal{L}_h^{c/a}[u_{\text{h},k}] - \mathcal{L}_h^{c/c}[u_k] - \mathcal{L}_h^{c/I}[u] + f_{\text{ext}}^c, \quad (49)$$

which can be directly obtained from (47). Now subtract (49) from $\mathcal{L}_h^{c/a}[u_{\text{ah},k+1}]$ leading to

$$\begin{aligned} \mathcal{L}_h^{c/a}[\Delta u_{\text{ah},k}] &= f_{\text{inh},k+1}^c = \mathcal{L}_h^{c/a}[u_{\text{ah},k+1}] + \mathcal{L}_h^{c/a}[u_{\text{h},k}] + \mathcal{L}_h^{c/c}[u_k] + \mathcal{L}_h^{c/I}[u] - f_{\text{ext}}^c \\ &= \mathcal{L}_h^{c/a}[u_{k+1}] + \mathcal{L}_h^{c/c}[u_k] + \mathcal{L}_h^{c/I}[u] - f_{\text{ext}}^c. \end{aligned} \quad (50)$$

which we denote as the *inhomogeneous force* $f_{\text{inh},k+1}$ in the $k+1$ -th iteration (cf., [12]). In the latter expression only the full solution appears and, therefore, $\mathcal{L}_h^{c/a}[\Delta u_{\text{ah},k}^a]$ can be evaluated conveniently after the anharmonic problem has been solved.

Remark 3. The name “inhomogeneous force” was coined in the original works by Sinclair (e.g., [30]). The origin of this name stems from the fact that updating the atomistic solution generates a mismatch between both models—which vanishes upon convergence. The idea of Sinclair was thus to update the displacements in Λ^c corresponding to a force which counteracts $\mathcal{L}_h^{c/a}[\Delta u_{\text{ah},k}^a]$; this is why the minus sign appears on the right hand side of (48).

In principle, the harmonic problem can be solved with any conventional finite element method. However, volume-based methods require a very fine discretization and can thus become significantly more expensive than the atomistic problem itself. For the class of A/C coupling problems, boundary element techniques seem preferable since the full solution in Λ^c is usually not explicitly required.

Therefore, We now formulate the implementation of (46) using the discrete boundary element method from Section 3.2. Algorithm 2 summarizes the proposed solution procedure. The algorithm is kept general and it should thus be noted that it suffices to compute the solution in the pad region $\Lambda^p \subset \Lambda^c$ in order to provide the boundary condition on the atomistic problem. The same holds for the external force f_{ext} .

6. Convergence analysis

We now analyze the convergence behavior of the Sinclair method. For this purpose, we linearize the coupled problem around a homogeneous displacement u_{F} , that is, we seek for a solution $u \in \mathcal{V}$ such that

$$\mathcal{L}_{\text{cpl}}(u_{\text{F}})[u - u_{\text{F}}] = \begin{cases} \mathcal{L}_{\text{hnl}}[u - u_{\text{F}}] = r_{\text{F}} & \text{in } \Lambda^a, \\ \mathcal{L}_{\text{h}}[u - u_{\text{F}}] = r_{\text{F}} & \text{in } \Lambda^c, \end{cases} \quad \text{where } r_{\text{F}} = f_{\text{ext}} - \mathcal{L}_{\text{cpl}}(u_{\text{F}})[u_{\text{F}}]. \quad (51)$$

This assumption, though restrictive, can be generalized in the sense that a nonlinear problem can also be considered as a sequence of linear problems. Moreover, in Section 7 we shall see that, using the tools from the linear analysis, we are able to improve the convergence behavior of general nonlinear problems by optimizing the transmission conditions between both problems around intermediate linearized states.

Algorithm 2: Sinclair method for bounded problems (Sinc)

Input: natural boundary condition \bar{u}^I , external force f_{ext}

- 1 **if** *initial guess* **then**
- 2 | $u_0^{\bar{A}} \leftarrow \text{DBEM}(\bar{u}^I, f_{\text{ext}})$;
- 3 **else**
- 4 | $u_0^{\bar{A}} \leftarrow 0$;
- 5 **end**
- 6 $k \leftarrow 0$;
- 7 **while** $\|\delta\Pi^a(u_k)\|_{l^\infty} < TOL \wedge \|\delta\Pi^c(u_k)\|_{l^\infty} < TOL$ **do**
- 8 | $u_{k+1}^a \leftarrow \arg \left\{ \min_{v^a} \Pi^a(\{v^a, u_k^p\}) \right\}$; // solve (AH)
- 9 | $f_{\text{inh},k+1}^c \leftarrow \mathcal{L}_h^{c/a}[u_{k+1}] + \mathcal{L}_h^{c/c}[u_k]$; // compute inhomogeneous force
- 10 | **if not** *initial guess* **and** $k = 0$ **then**
- 11 | | $u_k^{\bar{A}} \leftarrow \mathcal{G}^{\bar{A}/A}[f_{\text{ext}}]$;
- 12 | **end**
- 13 | $u_{k+1}^c \leftarrow u_k^c + \text{DBEM}(\bar{u}^I - u_k^I, -f_{\text{inh},k+1}^c)$; // solve (H)
- 14 | $k \leftarrow k + 1$;
- 15 **end**

Output: global solution u_k

Our analysis is closely related to projection-based domain decomposition [33]. That is, we first derive a projection operator which maps the error in the $k+1$ -th iteration to the error in the $k+2$ -th iteration. Subsequently, in Section 6.2 and 6.3, we analyze the stability of Algorithm 2 based on the spectral properties of the projection operator.

6.1. Projection operator

Below, we frequently make use of the following quantities,

- the Schur complement of $\mathcal{L}_h^{a/a}$ in \mathcal{L}_{cpl}

$$\mathcal{S}^{c/c} = \mathcal{L}_h^{c/c} - \mathcal{L}_h^{c/a}(\mathcal{L}_h^{a/a})^{-1}\mathcal{L}_h^{a/c} \quad (\equiv \mathcal{L}_{\text{cpl}}/\mathcal{L}_h^{a/a}), \quad (52)$$

- and the boundary operator

$$\mathcal{B}^{c/I} = \mathcal{F}^{c/I} + \mathcal{G}^{c/I}\mathcal{G}^{I/I-1}(\mathcal{I}^{I/I} - \mathcal{F}^{I/I}) \quad (53)$$

which maps a boundary displacement v^I to the solution in Λ^c (this operation corresponds to $\text{DBEM}(v^I, 0)$).

In addition, we define the set of atoms which interact with continuum nodes as $\Lambda^{P'} = \{-M, -M+1, M-1, M\}$. A corresponding operator with domain $\mathcal{V}(\Lambda^{P'})$ and, e.g., codomain $\mathcal{V}(\Lambda^P)$, is thus defined as $\mathcal{T}^{P'/P} : \mathcal{V}(\Lambda^{P'}) \rightarrow \mathcal{V}(\Lambda^P)$.

Using the previous definitions, we now state the first main result of Section 6:

Lemma 1 (Projection operator). *Let u be a unique solution to (40). Then, Algorithm 2 can be written as a projection method, that is,*

$$u_{k+1} - u = \mathcal{P}[u_k - u] \quad \text{in } \Lambda, \quad (54)$$

with the projection operator $\mathcal{P} : \mathcal{V} \rightarrow \mathcal{V}$ given by

$$\mathcal{P} = \begin{pmatrix} \mathcal{P}^{a/a} & \mathcal{P}^{a/c} \\ \mathcal{P}^{c/a} & \mathcal{P}^{c/c} \end{pmatrix} = \begin{pmatrix} \mathbf{0}^{a/a} & \mathcal{L}_{\text{hnl}}^{a/a-1}\mathcal{L}_{\text{hnl}}^{a/c} \\ \mathbf{0}^{c/a} & \mathcal{I}^{c/c} - \mathcal{S}^{c/c-1}(\mathcal{L}_h^{c/c} - \mathcal{L}_h^{c/a}\mathcal{L}_{\text{hnl}}^{a/a-1}\mathcal{L}_{\text{hnl}}^{a/c}) \end{pmatrix}. \quad (55)$$

Moreover, according to Algorithm 2, line 8 and 13, the operators $\mathcal{P}^{c/a}$ and $\mathcal{P}^{c/c}$ can be written as

$$\mathcal{P}^{a/c} = \begin{pmatrix} \mathcal{P}^{a/p} & \mathbf{0}^{a/c \setminus p} \end{pmatrix}, \quad \text{with } \mathcal{P}^{a/p} = (\mathcal{L}_{\text{hnl}}^{a/a-1})^{a/p'} \mathcal{L}_{\text{hnl}}^{p'/p}, \quad (56)$$

$$\mathcal{P}^{c/c} = \begin{pmatrix} \mathcal{P}^{c/p} & \mathbf{0}^{c/c \setminus p} \end{pmatrix}, \quad \text{with } \mathcal{P}^{c/p} = \mathcal{P}_1^{c/p} + \mathcal{P}_2^{c/p}, \quad (57)$$

where

$$\mathcal{P}_1^{c/p} = (\mathcal{G}^{c/i} - \mathcal{B}^{c/I} \mathcal{G}^{I/i}) \mathcal{L}_h^{i/p}, \quad \mathcal{P}_2^{c/p} = (\mathcal{G}^{c/i+} - \mathcal{B}^{c/I} \mathcal{G}^{I/i+}) \mathcal{L}_h^{i+/i} (\mathcal{L}_{\text{hnl}}^{a/a-1})^{i/p'} \mathcal{L}_{\text{hnl}}^{p'/p}. \quad (58)$$

PROOF. The proof is conducted in two steps: first, the iterate $u_{k+1} - u$ is derived in terms of the global projection operator (55). In the second step we will prove (56) and (57).

To avoid further technicalities, we assume that $k > 1$ such that the contributions due to the boundary conditions and the external force are already contained in u_1 .

Step 1

We begin by writing the global solution $u_{k+1/2}$ after Algorithm 2, line 8, as

$$\begin{aligned} u_{k+1/2} &= \begin{pmatrix} u_{k+1/2}^a \\ u_{k+1/2}^c \end{pmatrix} = \begin{pmatrix} u_k^a \\ u_k^c \end{pmatrix} = \begin{pmatrix} u_k^a \\ u_k^c \end{pmatrix} + \begin{pmatrix} \mathcal{L}_{\text{hnl}}^{a/a-1} & \mathbf{0}^{a/c} \\ \mathbf{0}^{c/a} & \mathbf{0}^{c/c} \end{pmatrix} \begin{pmatrix} f_{\text{ext}}^a - \mathcal{L}_{\text{hnl}}^a[u_k] \\ f_{\text{ext}}^c - \mathcal{L}_h^c[u_k] \end{pmatrix} \\ &= \begin{pmatrix} u_k^a \\ u_k^c \end{pmatrix} + \begin{pmatrix} \mathcal{L}_{\text{hnl}}^{a/a-1} & \mathbf{0}^{a/c} \\ \mathbf{0}^{c/a} & \mathbf{0}^{c/c} \end{pmatrix} \begin{pmatrix} \mathcal{L}_{\text{hnl}}^{a/a} & \mathcal{L}_{\text{hnl}}^{a/c} \\ \mathcal{L}_h^{c/a} & \mathcal{L}_h^{c/c} \end{pmatrix} \begin{bmatrix} u^a - u_k^a \\ u^c - u_k^c \end{bmatrix} \\ &= \begin{pmatrix} u_k^a \\ u_k^c \end{pmatrix} + \begin{pmatrix} \mathcal{I}^{a/a} & \mathcal{L}_{\text{hnl}}^{a/a-1} \mathcal{L}_{\text{hnl}}^{a/c} \\ \mathbf{0}^{c/a} & \mathbf{0}^{c/c} \end{pmatrix} \begin{bmatrix} u^a - u_k^a \\ u^c - u_k^c \end{bmatrix}. \end{aligned} \quad (59)$$

Analogously, we can write the global solution u_{k+1} after Algorithm 2, line 13, as

$$\begin{aligned} u_{k+1} &= \begin{pmatrix} u_{k+1}^a \\ u_{k+1}^c \end{pmatrix} = \begin{pmatrix} u_{k+1/2}^a \\ u_{k+1/2}^c \end{pmatrix} + \begin{pmatrix} \mathbf{0}^{a/a} & \mathbf{0}^{a/c} \\ \mathbf{0}^{c/a} & \mathcal{S}^{c/c-1} \end{pmatrix} \begin{pmatrix} f_{\text{ext}}^a - \mathcal{L}_{\text{hnl}}^a[u_{k+1/2}] \\ f_{\text{ext}}^c - \mathcal{L}_h^c[u_{k+1/2}] \end{pmatrix} \\ &= \begin{pmatrix} u_{k+1/2}^a \\ u_{k+1/2}^c \end{pmatrix} + \begin{pmatrix} \mathbf{0}^{a/a} & \mathbf{0}^{a/c} \\ \mathbf{0}^{c/a} & \mathcal{S}^{c/c-1} \end{pmatrix} \begin{pmatrix} \mathcal{L}_{\text{hnl}}^{a/a} & \mathcal{L}_{\text{hnl}}^{a/c} \\ \mathcal{L}_h^{c/a} & \mathcal{L}_h^{c/c} \end{pmatrix} \begin{bmatrix} u^a - u_{k+1/2}^a \\ u^c - u_{k+1/2}^c \end{bmatrix} \\ &= \begin{pmatrix} u_{k+1/2}^a \\ u_{k+1/2}^c \end{pmatrix} + \begin{pmatrix} \mathbf{0}^{a/a} & \mathbf{0}^{a/c} \\ \mathcal{S}^{c/c-1} \mathcal{L}_h^{c/a} & \mathcal{S}^{c/c-1} \mathcal{L}_h^{c/c} \end{pmatrix} \begin{bmatrix} u^a - u_{k+1/2}^a \\ u^c - u_{k+1/2}^c \end{bmatrix}. \end{aligned} \quad (60)$$

Thus, we can write the multiplicative iterates as

$$u_{k+1/2} = u_k + \mathcal{P}_a[u - u_k] \quad \text{in } \Lambda, \quad (61)$$

$$u_k = u_{k+1/2} + \mathcal{P}_c[u - u_{k+1/2}] \quad \text{in } \Lambda, \quad (62)$$

with the projection operators

$$\mathcal{P}_a = \begin{pmatrix} \mathcal{I}^{a/a} & \mathcal{L}_{\text{hnl}}^{a/a-1} \mathcal{L}_{\text{hnl}}^{a/c} \\ \mathbf{0}^{c/a} & \mathbf{0}^{c/c} \end{pmatrix}, \quad \mathcal{P}_c = \begin{pmatrix} \mathbf{0}^{a/a} & \mathbf{0}^{a/c} \\ \mathcal{S}^{c/c-1} \mathcal{L}_h^{c/a} & \mathcal{S}^{c/c-1} \mathcal{L}_h^{c/c} \end{pmatrix}. \quad (63)$$

Using (61) in (62) now permits to obtain (54)

$$u_{k+1} - u = \mathcal{P}[u_k - u] \quad \text{in } \Lambda \quad (64)$$

since

$$\begin{aligned} \mathcal{P} &= \mathcal{I} - \mathcal{P}_a - \mathcal{P}_c + \mathcal{P}_c \mathcal{P}_a \\ &= \begin{pmatrix} \mathbf{0}^{a/a} & \mathcal{L}_{\text{hnl}}^{a/a-1} \mathcal{L}_{\text{hnl}}^{a/c} \\ \mathbf{0}^{c/a} & \mathcal{I}^{c/c} - \mathcal{S}^{c/c-1} (\mathcal{L}_h^{c/c} - \mathcal{L}_h^{c/a} \mathcal{L}_{\text{hnl}}^{a/a-1} \mathcal{L}_{\text{hnl}}^{a/c}) \end{pmatrix}. \end{aligned} \quad (65)$$

Step 2

It is straightforward to see that

$$\mathcal{P}^{A/c} = \begin{pmatrix} \mathcal{P}^{A/P} & \mathbf{0}^{A/c \setminus P} \end{pmatrix} \quad (66)$$

since $\forall v \in \mathcal{V}$ it holds

$$\mathcal{L}_{\text{hnl}}^{a/c \setminus P}[v] = 0 \quad \text{in } A^a, \quad \mathcal{L}_{\text{hnl}}^{a/P}[v] = 0 \quad \text{in } A^a \setminus A^{P'}. \quad (67)$$

Moreover, equation (67) also implies that

$$\mathcal{P}^{a/P} = \mathcal{L}_{\text{hnl}}^{a/a-1} \mathcal{L}_{\text{hnl}}^{a/P} = (\mathcal{L}_{\text{hnl}}^{a/a-1})^{a/P'} \mathcal{L}_{\text{hnl}}^{P'/P}, \quad (68)$$

which yields (56).

It remains to analyze the operator $\mathcal{P}^{c/P}$. For this purpose, we first recall that the inverse of the Schur complement $\mathcal{S}^{c/c}$ can be written as

$$\mathcal{S}^{c/c-1} = \mathcal{G}^{c/c} - \mathcal{B}^{c/I} \mathcal{G}^{I/c}. \quad (69)$$

In addition, we note that the block $(\mathcal{G}\mathcal{L}_h)^{c/P}$ from (30) can likewise be given as

$$\begin{aligned} (\mathcal{G}\mathcal{L}_h)^{c/P} &= \mathcal{I}^{c/P} = \mathcal{G}^{c/\bar{\lambda}} \mathcal{L}_h^{\bar{\lambda}/P} + \underbrace{\mathcal{G}^{c/r} \mathcal{L}_h^{r/P}}_{=\mathbf{0}^{c/P}} \\ &= \mathcal{G}^{c/a} \mathcal{L}_h^{a/P} + \mathcal{G}^{c/c} \mathcal{L}_h^{c/P} + \mathcal{G}^{c/I} \mathcal{L}_h^{I/P} \\ &\stackrel{(31)}{=} \mathcal{G}^{c/i} \mathcal{L}_h^{i/P} + \mathcal{G}^{c/c} \mathcal{L}_h^{c/P} + \mathcal{G}^{c/I} \mathcal{L}_h^{I/P}. \end{aligned} \quad (70)$$

Using $\mathcal{G}^{c/c} \mathcal{L}_h^{c/P} = \mathcal{I}^{c/P} - \mathcal{G}^{c/i} \mathcal{L}_h^{i/P} - \mathcal{G}^{c/I} \mathcal{L}_h^{I/P}$ and (69) in (65), we can write

$$\mathcal{P}^{c/P} = \mathcal{G}^{c/i} \mathcal{L}_h^{i/P} + \mathcal{G}^{c/I} \mathcal{L}_h^{I/P} + \mathcal{B}^{c/I} \mathcal{G}^{I/c} \mathcal{L}_h^{c/P} + (\mathcal{G}^{c/c} - \mathcal{B}^{c/I} \mathcal{G}^{I/c}) \mathcal{L}_h^{c/a} (\mathcal{L}_{\text{hnl}}^{a/a-1})^{a/P'} \mathcal{L}_{\text{hnl}}^{a/P'/P}. \quad (71)$$

Next, we analyze the second and third term of (71). Again, using (30), we can rewrite the block $(\mathcal{G}\mathcal{L}_h)^{I/P}$ as follows

$$(\mathcal{G}\mathcal{L}_h)^{I/P} = \mathcal{G}^{I/i} \mathcal{L}_h^{i/P} + \mathcal{G}^{I/c} \mathcal{L}_h^{c/P} + \mathcal{G}^{I/I} \mathcal{L}_h^{I/P} = \mathbf{0}^{I/P}. \quad (72)$$

With $\mathcal{G}^{I/c} \mathcal{L}_h^{c/P} = -\mathcal{G}^{I/i} \mathcal{L}_h^{i/P} - \mathcal{G}^{I/I} \mathcal{L}_h^{I/P}$, it follows

$$\begin{aligned} \mathcal{G}^{c/I} \mathcal{L}_h^{I/P} + \mathcal{B}^{c/I} \mathcal{G}^{I/c} \mathcal{L}_h^{c/P} &= \mathcal{G}^{c/I} \mathcal{L}_h^{I/P} - \mathcal{B}^{c/I} \mathcal{G}^{I/I} \mathcal{L}_h^{I/P} - \mathcal{B}^{c/I} \mathcal{G}^{I/i} \mathcal{L}_h^{i/P} \\ &= -\mathcal{B}^{c/I} \mathcal{G}^{I/i} \mathcal{L}_h^{i/P} \end{aligned} \quad (73)$$

since $\mathcal{G}^{c/I} \mathcal{L}_h^{I/P} - \mathcal{B}^{c/I} \mathcal{G}^{I/I} \mathcal{L}_h^{I/P} = \mathbf{0}^{c/P}$, which follows from the fact that, for any input, both operators produce the same solution in A^c . Finally, using the following properties of \mathcal{L}_h , i.e., $\forall v \in \mathcal{V}$

$$\mathcal{L}_h^{c/a \setminus i}[v] = 0 \quad \text{in } A^c, \quad \mathcal{L}_h^{c/i}[v] = 0 \quad \text{in } A^c \setminus A^{i+}, \quad (74)$$

we can write the last term of (71) as

$$(\mathcal{G}^{c/c} - \mathcal{B}^{c/I} \mathcal{G}^{I/c}) \mathcal{L}_h^{c/a} (\mathcal{L}_{\text{hnl}}^{a/a-1})^{a/P'} \mathcal{L}_{\text{hnl}}^{P'/P} = (\mathcal{G}^{c/i+} - \mathcal{B}^{c/I} \mathcal{G}^{I/i+}) \mathcal{L}_h^{i+/i} (\mathcal{L}_{\text{hnl}}^{a/a-1})^{i/P'} \mathcal{L}_{\text{hnl}}^{P'/P}. \quad (75)$$

Using (73) and (75) in (71), we obtain

$$\mathcal{P}^{c/p} = \mathcal{G}^{c/i} \mathcal{L}_h^{i/p} - \mathcal{B}^{c/I} \mathcal{G}^{I/i} \mathcal{L}_h^{i/p} + (\mathcal{G}^{c/i+} - \mathcal{B}^{c/I} \mathcal{G}^{I/i+}) \mathcal{L}_h^{i+/i} (\mathcal{L}_{\text{hnl}}^{a/a-1})^{i/p'} \mathcal{L}_{\text{hnl}}^{p'/p}, \quad (76)$$

which proves (55). \square

It will prove useful in the following to split the operator into a contribution due to the inhomogeneous problem and the homogeneous finite problem such that

$$\mathcal{P} = \tilde{\mathcal{P}} + \hat{\mathcal{P}} = \begin{pmatrix} \mathbf{0}^{a/a} & \mathcal{P}^{a/p} & \mathbf{0}^{a/c \setminus p} \\ \mathbf{0}^{c/a} & \tilde{\mathcal{P}}^{c/p} & \mathbf{0}^{c/c \setminus p} \end{pmatrix} + \begin{pmatrix} \mathbf{0}^{a/a} & \mathbf{0}^{a/p} & \mathbf{0}^{a/c \setminus p} \\ \mathbf{0}^{c/a} & \hat{\mathcal{P}}^{c/p} & \mathbf{0}^{c/c \setminus p} \end{pmatrix}, \quad (77)$$

where

$$\tilde{\mathcal{P}}^{c/p} = \mathcal{G}^{c/i} \mathcal{L}_h^{i/p} + \mathcal{G}^{c/i+} \mathcal{L}_h^{i+/i} (\mathcal{L}_{\text{hnl}}^{a/a-1})^{i/p'} \mathcal{L}_{\text{hnl}}^{p'/p}, \quad (78)$$

$$\hat{\mathcal{P}}^{c/p} = -\mathcal{B}^{c/I} \mathcal{G}^{I/i} \mathcal{L}_h^{i/p} - \mathcal{B}^{c/I} \mathcal{G}^{I/i+} \mathcal{L}_h^{i+/i} (\mathcal{L}_{\text{hnl}}^{a/a-1})^{i/p'} \mathcal{L}_{\text{hnl}}^{p'/p}. \quad (79)$$

Note that the latter vanishes for infinite problems.

6.2. Convergence rate

We are now in the position to prove the convergence rate of the Sinclair method:

Theorem 1 (Convergence rate). *Under the assumption that the projection operator \mathcal{P} admits the eigendecomposition $\mathcal{P} = \mathcal{Q}\mathcal{D}\mathcal{Q}^{-1}$ the norm of the error in the $k+1$ -th iteration can be bounded from above as*

$$\|u_{k+1} - u\| \leq \sigma^{k+1} \|\mathcal{Q}\| \|\mathcal{Q}^{-1}\| \|u_0 - u\|, \quad (80)$$

where $\sigma = \sigma(\mathcal{P})$ is the spectral radius of \mathcal{P} . Moreover, the spectral radius of \mathcal{P} is equivalent to the spectral radius of $\mathcal{P}^{p/p}$, that is, $\sigma = \sigma(\mathcal{P}^{p/p})$.

PROOF. Using (54), we can write the iterates until the $k+1$ -th iteration as

$$u_1 - u = \mathcal{P}[u_0 - u] \quad \text{in } \Lambda, \quad (81)$$

\vdots

$$u_{k+1} - u = \mathcal{P}[u_k - u] \quad \text{in } \Lambda. \quad (82)$$

Recursively using the error from the previous iteration(s) in (82). we obtain

$$u_{k+1} - u = \mathcal{P}^{k+1}[u_0 - u], \quad \text{where } \mathcal{P}^{k+1} = \prod_{i=1}^{k+1} \mathcal{P}_i = \mathcal{Q}\mathcal{D}\mathcal{Q}^{-1}\mathcal{Q}\mathcal{D}\mathcal{Q}^{-1} \dots = \mathcal{Q}\mathcal{D}^{k+1}\mathcal{Q}^{-1}. \quad (83)$$

Taking norms on both sides and using the Cauchy-Schwarz inequality, we obtain the expected bound.

The second statement is obtained by rewriting \mathcal{P} as an upper triangular block matrix by inverting the Λ^p and $\Lambda^{c \setminus p}$ entries. The spectral radius of this upper triangular matrix is equivalent to the spectral radius of its diagonal block which is nothing but $\mathcal{P}^{p/p}$. \square

For the special case when the atomistic and continuum models coincide, the exact number of required iterations can be immediately deduced from Theorem 1:

Corollary 1. *Let $\mathcal{L}_{\text{hnl}}^a = \mathcal{L}_h^a$ such that $\mathcal{L}_{\text{cpl}} = \mathcal{L}_h$. Then, Algorithm 2 converges in two steps.*

PROOF. It suffices to show that the projection operator vanishes. Indeed, since $\mathcal{S}^{c/c-1}$ is now nothing but the inverse of the Schur complement $\mathcal{L}_{\text{cpl}}/\mathcal{L}_h^{a/a} = \mathcal{L}_h^{c/c} - \mathcal{L}_h^{c/a} (\mathcal{L}_h^{a/a})^{-1} \mathcal{L}_h^{a/c}$ (cf., [37]) it follows immediately that

$$\mathcal{P}^{c/c} = \mathcal{I}^{c/c} - \mathcal{S}^{c/c-1} (\mathcal{L}_{\text{cpl}}/\mathcal{L}_h^{a/a}) = 0 \quad (84)$$

and, therefore, $u_2 - u = 0$. \square

This result is general and holds for arbitrary interaction stencils—provided that we can compute the corresponding lattice Green function.

Moreover, for the one-dimensional system we can show that the convergence rate only depends on the spectral properties of the inhomogeneous operator $\tilde{\mathcal{P}}$:

Proposition 1. *For the one-dimensional system the convergence rate does not depend on the boundary operator (53), that is,*

$$\|u_{k+1} - u\| \leq C_1 \max\{\tilde{\sigma}^{k+1}, C_2 \tilde{\sigma}^k\} \|u_0 - u\|, \quad (85)$$

where $\tilde{\sigma}$ is the spectral radius of $\tilde{\mathcal{P}}$ and $C_1, C_2 > 0$ are constants, independent of k .

PROOF. We recall that the projection operator is given in the $k+1$ -th iteration by

$$\mathcal{P}^{k+1} = \prod_{i=1}^{k+1} \mathcal{P}_i = \prod_{i=1}^{k+1} (\tilde{\mathcal{P}}_i + \hat{\mathcal{P}}_i) = (\tilde{\mathcal{P}} + \hat{\mathcal{P}})(\tilde{\mathcal{P}} + \hat{\mathcal{P}}) \dots = (\tilde{\mathcal{P}}^2 + \tilde{\mathcal{P}}\hat{\mathcal{P}} + \hat{\mathcal{P}}\tilde{\mathcal{P}} + \hat{\mathcal{P}}^2) \dots \quad (86)$$

We first analyze successive applications of $\hat{\mathcal{P}}$ to itself. Therefore, first note that an application of an arbitrary vector $v \in \mathcal{V}$ gives a homogeneous solution $w(\xi) = F\xi + C$, for some $F, C > 0$ since the homogeneous problem does not contain any source terms. Since the coupling is consistent, applying homogeneous boundary conditions $u^p = w^p$ to the atomistic problem gives the same solution in Λ^a , i.e., $(\mathcal{L}^{a/a} \mathcal{L}^{a/c})[w] = w^a$, and, therefore, $\mathcal{L}^{c/c}[w] - \mathcal{L}^{c/a}[w] = 0$. This implies

$$\forall v \in \mathcal{V} \quad (\hat{\mathcal{P}}\hat{\mathcal{P}})[v] = 0 \quad (87)$$

which can only hold if $\hat{\mathcal{P}}\hat{\mathcal{P}} = \mathbf{0}$. That is, the operator $\hat{\mathcal{P}}$ is nilpotent with index 2.

In addition, since $\hat{\mathcal{P}}$ generates homogeneous solutions, the inhomogeneous force vanishes and, therefore, it also holds $\tilde{\mathcal{P}}\hat{\mathcal{P}} = \mathbf{0}$.

With $\hat{\mathcal{P}}\hat{\mathcal{P}} = \tilde{\mathcal{P}}\hat{\mathcal{P}} = \mathbf{0}$, equation (86) reduces to

$$\mathcal{P}^{k+1} = \tilde{\mathcal{P}}^{k+1} + \hat{\mathcal{P}}\tilde{\mathcal{P}}^k. \quad (88)$$

Assuming that $\tilde{\mathcal{P}}^{k+1}$ has the eigendecomposition $\tilde{\mathcal{P}}^{k+1} = \tilde{\mathcal{Q}}\tilde{\mathcal{D}}^{k+1}\tilde{\mathcal{Q}}^{-1}$, we can write (88) as

$$u_{k+1} - u = (\tilde{\mathcal{Q}}\tilde{\mathcal{D}}^{k+1}\tilde{\mathcal{Q}}^{-1} + \hat{\mathcal{P}}\tilde{\mathcal{Q}}\tilde{\mathcal{D}}^k\tilde{\mathcal{Q}}^{-1})[u_0 - u] \quad (89)$$

from which the upper bound follows as

$$\|u_{k+1} - u\| \leq (\tilde{\sigma}^{k+1} + \tilde{\sigma}^k \|\hat{\mathcal{P}}\|) \|\tilde{\mathcal{Q}}\| \|\tilde{\mathcal{Q}}^{-1}\| \|u_0 - u\|. \quad (90)$$

With $C_1 = \|\tilde{\mathcal{Q}}\| \|\tilde{\mathcal{Q}}^{-1}\|$ and $C_2 = \|\hat{\mathcal{P}}\|$ we obtain (85). \square

It would be interesting if this result can be generalized to higher dimensions. If it holds, at least in an approximate way, it may suffice to analyze the convergence properties of the Sinclair algorithm using only the artificial boundary data. This would simplify the computation of relaxation factors in order to improve the convergence rate (cf., Section 6.4 and 7).

6.3. Stability

We now turn to the question whether the Sinclair method is stable, that is, under which conditions $\sigma(\mathcal{P}^{p/p}) < 1$ holds for the general case when $\mathcal{L}_h \neq \mathcal{L}_{\text{hnl}}$.

A general stability estimate requires precise knowledge of the atomistic operator $\mathcal{L}^{a/a}$. Therefore, attention is drawn to a system with pairwise second nearest neighbor interactions which has been extensively studied by Dobson et al. [5] who reported physical restrictions on the choice of the force constants. That is, we consider the stencil

$$K_{\text{hnl}}(\xi - \eta) = \begin{cases} -k_2 & \text{if } |\xi - \eta| = 2a_0, \\ -k_1 & \text{if } |\xi - \eta| = a_0, \\ 2k & \text{if } |\xi - \eta| = 0, \\ 0 & \text{else,} \end{cases} \quad (91)$$

where $k = k_1 + k_2$. The corresponding Euler-Lagrange equation then reads

$$\mathcal{L}_{\text{cpl}}[u](\xi) = \begin{cases} -k_2(u(\xi - 2a_0) - 2u(\xi) + u(\xi + 2a_0)) - k_1(u(\xi - a_0) - 2u(\xi) + u(\xi + a_0)) = f_{\text{ext}}(\xi) & \forall \xi \in \Lambda^a, \\ -\bar{k}(u(\xi - a_0) - 2u(\xi) + u(\xi + a_0)) = f_{\text{ext}}(\xi) & \forall \xi \in \Lambda^c, \end{cases} \quad (92)$$

with $\bar{k} = k_1 + 4k_2$. Following Dobson et al. [5], we assume that $k_1 > 0$ and $k_2 < 0$ which yields the condition $k_1 + 4k_2 > 0$ to render $\mathcal{L}^{a/a}$ positive definite and (92) a well-posed problem.

The author is aware of one related stability result by Parks et al. [22] who proved that the alternating Schwarz method is stable by showing, i.a., that the projection operator is strictly positive, i.e., $\mathcal{P} > 0$, meaning that all entries of its corresponding matrix are positive. However, the proof in [22] assumes that the atomistic Hessian is an M -matrix.¹ This is generally not the case since its off-diagonal components are positive *and* negative for physically admissible interatomic potentials (see above). Unfortunately, even if \mathcal{L} is an M -matrix, the operator \mathcal{P} is not strictly positive. To see this, fix a $C > 0$ such that $\mathcal{G}^{c/i}, \mathcal{G}^{c/i^*} > 0$. Now consider \mathcal{P} from (65) factorized to

$$\mathcal{P} = (\mathcal{I} - \mathcal{P}_c)(\mathcal{I} - \mathcal{P}_a). \quad (93)$$

Since \mathcal{L}_h is always an M -matrix (since $\bar{k} > 0$), we have that $\mathcal{S}^{c/c^{-1}} > 0$. Therefore, $(\mathcal{I} - \mathcal{P}_c) \not> 0$. Since $(\mathcal{I} - \mathcal{P}_a) > 0$, it follows that $\mathcal{P} \not> 0$, in general, which has also been observed in numerical experiments.

Fortunately, for the one-dimensional system, it is feasible to estimate the spectral radius directly which allows us to establish the following theorem:

Theorem 2 (Stability). *Let \mathcal{L}_{cpl} be given by (92). Then, Algorithm 2 is unconditionally stable in the sense that*

$$\sigma(\mathcal{P}^{\text{p/p}}) = \sigma(\tilde{\mathcal{P}}^{\text{p/p}}) < 1. \quad (94)$$

The idea is to estimate $\sigma(\mathcal{P}^{\text{p/p}})$ by without explicitly computing the inverse of the atomistic Hessian. However, we still require the following preliminary result concerning estimates of the coefficients of $\underline{\underline{L}}^{a/a^{-1}}$:

Proposition 2. *Let $\mathcal{L}^{a/a}$ be given by (92) and*

$$\underline{\underline{L}}^{a/a} = \begin{pmatrix} L^{a/a}(-M, -M) & \cdots & L^{a/a}(-M, M) \\ \vdots & \ddots & \vdots \\ L^{a/a}(M, -M) & \cdots & L^{a/a}(M, M) \end{pmatrix} \quad (95)$$

be its matrix representation. With $k_2 \in (-k_1/4, 0)$ it then holds

(a) *Positivity of the inverse coefficients:* $L_{1,1}^{a/a^{-1}}, L_{1,N^a}^{a/a^{-1}} > 0$.

(b) *Ratio of the inverse coefficients:*

$$(b.1) \quad \frac{L_{1,N^a-1}^{a/a^{-1}}}{L_{1,N^a}^{a/a^{-1}}} < 3 - \frac{3}{2M+1}, \quad (b.2) \quad \frac{L_{1,1}^{a/a^{-1}}}{L_{1,N^a}^{a/a^{-1}}} > 1.$$

PROOF. The proof is subjected to Appendix A.

With this result we can now prove Theorem 2:

PROOF (OF THEOREM 2). The equality in (94) follows directly from Proposition 1. Therefore, we begin by defining the projection matrix corresponding to $\tilde{\mathcal{P}}^{\text{p/p}}$ as

$$\underline{\underline{\tilde{\mathcal{P}}}}^{\text{p/p}} = \begin{pmatrix} \tilde{P}(-M, -M) & \tilde{P}(-M, -M+1) & \tilde{P}(-M, M-1) & \tilde{P}(-M, M) \\ \tilde{P}(-M+1, -M) & \tilde{P}(-M+1, -M+1) & \tilde{P}(-M+1, M-1) & \tilde{P}(-M+1, M) \\ \tilde{P}(M-1, -M) & \tilde{P}(M-1, -M+1) & \tilde{P}(M-1, M-1) & \tilde{P}(M-1, M) \\ \tilde{P}(M, -M) & \tilde{P}(M, -M+1) & \tilde{P}(M, M-1) & \tilde{P}(M, M) \end{pmatrix}. \quad (96)$$

¹A nonsingular matrix $\underline{\underline{L}} \in \mathbb{R}^{N \times N}$ is an M -matrix if its off-diagonal components are nonpositive and its inverse is nonnegative (cf., [24])

Using the interactions stencils (92) and the Green function (26), the individual coefficients read

$$\begin{aligned}
\tilde{P}_{1,1} &= \tilde{P}_{4,4} = -k_2(L_{1,1}^{a/a^{-1}} + (2M+3)L_{1,N^a}^{a/a^{-1}})/2, \\
\tilde{P}_{1,2} &= \tilde{P}_{4,3} = -k_1(L_{1,1}^{a/a^{-1}} + (2M+3)L_{1,N^a}^{a/a^{-1}})/2 - k_2(L_{1,2}^{a/a^{-1}} + (2M+3)L_{1,N^{a-1}}^{a/a^{-1}})/2 + 1, \\
\tilde{P}_{1,3} &= \tilde{P}_{4,2} = -k_1((2M+3)L_{1,1}^{a/a^{-1}} + L_{1,N^a}^{a/a^{-1}})/2 - k_2((2M+3)L_{1,2}^{a/a^{-1}} + L_{1,N^{a-1}}^{a/a^{-1}})/2 + M + 1, \\
\tilde{P}_{1,4} &= \tilde{P}_{4,1} = -k_2((2M+3)L_{1,N^a}^{a/a^{-1}} + L_{1,N^a}^{a/a^{-1}})/2, \\
\tilde{P}_{2,1} &= \tilde{P}_{3,4} = -(M+1)k_2L_{1,N^a}^{a/a^{-1}}, \\
\tilde{P}_{2,2} &= \tilde{P}_{3,3} = -(M+1)k_2L_{1,N^{a-1}}^{a/a^{-1}} - (M+1)k_1L_{1,N^a}^{a/a^{-1}} + 1/2, \\
\tilde{P}_{2,3} &= \tilde{P}_{3,2} = -(M+1)k_1L_{1,1}^{a/a^{-1}} - (M+1)k_2L_{1,2}^{a/a^{-1}} + M + 1/2, \\
\tilde{P}_{2,4} &= \tilde{P}_{3,1} = -(M+1)k_2L_{1,1}^{a/a^{-1}}.
\end{aligned} \tag{97}$$

Using (97), it can be readily shown that the projection matrix has rank 2. Moreover, $\underline{\tilde{P}}^{p/p}$ is centrosymmetric and, therefore, its spectrum are the eigenvalues of (cf., [3])

$$\underline{\underline{C}}_1 = \begin{pmatrix} \tilde{P}_{1,1} - \tilde{P}_{1,4} & \tilde{P}_{1,2} - \tilde{P}_{1,3} \\ \tilde{P}_{2,1} - \tilde{P}_{2,4} & \tilde{P}_{2,2} - \tilde{P}_{2,3} \end{pmatrix}, \quad \underline{\underline{C}}_2 = \begin{pmatrix} \tilde{P}_{1,1} + \tilde{P}_{1,4} & \tilde{P}_{1,2} + \tilde{P}_{1,3} \\ \tilde{P}_{2,1} + \tilde{P}_{2,4} & \tilde{P}_{2,2} + \tilde{P}_{2,3} \end{pmatrix}. \tag{98}$$

From (97) it follows $\tilde{P}_{1,1} - \tilde{P}_{1,4} = \tilde{P}_{2,1} - \tilde{P}_{2,4}$ and $\tilde{P}_{1,2} - \tilde{P}_{1,3} = \tilde{P}_{2,2} - \tilde{P}_{2,3}$. The eigenvalues of $\underline{\underline{C}}_1$ are then given by

$$\lambda_{11} = (\tilde{P}_{1,1} - \tilde{P}_{1,4}) + (\tilde{P}_{1,2} - \tilde{P}_{1,3}), \quad \lambda_{12} = 0. \tag{99}$$

Hence, at least one eigenvalue of $\underline{\underline{C}}_2$ must be equal to zero which implies that the possibly nonzero eigenvalue is given by the trace of $\underline{\underline{C}}_2$. Thus, the eigenvalues of $\underline{\underline{C}}_2$ are

$$\lambda_{21} = (\tilde{P}_{1,1} + \tilde{P}_{1,4}) + (\tilde{P}_{2,2} + \tilde{P}_{2,3}), \quad \lambda_{22} = 0. \tag{100}$$

Exploiting the identity

$$-(M+1)(k_1(L_{1,1}^{a/a^{-1}} - L_{1,N^a}^{a/a^{-1}}) + k_2(L_{1,2}^{a/a^{-1}} - L_{1,N^{a-1}}^{a/a^{-1}})) - (M+2)k_2(k_1(L_{1,1}^{a/a^{-1}} - L_{1,N^a}^{a/a^{-1}})) = -M, \tag{101}$$

which can be obtained by applying a homogeneous deformation to the crystal, the eigenvalues can be written as

$$\lambda_{11} = -k_2(L_{1,1}^{a/a^{-1}} + L_{1,N^a}^{a/a^{-1}}) + 2k_2L_{1,N^a}^{a/a^{-1}}, \tag{102}$$

$$\lambda_{21} = -k_2(L_{1,1}^{a/a^{-1}} + L_{1,N^a}^{a/a^{-1}}), \tag{103}$$

from which it follows that $\lambda_{11} < \lambda_{21}$. Using the statements (a) and (b.2) from Proposition 2, we immediately find that $\lambda_{11} > 0$ and, therefore, it remains to check whether $\lambda_{21} = \sigma < 1$.

For this purpose, using the identities (101) and

$$(k_1 + k_2)(L_{1,1}^{a/a^{-1}} + L_{1,N^a}^{a/a^{-1}}) + k_2(L_{1,2}^{a/a^{-1}} + L_{1,N^{a-1}}^{a/a^{-1}}) = 1 \tag{104}$$

in (103), λ_{21} becomes

$$\begin{aligned}
\lambda_{21} &= (M+1) \left(1 - 2 \left(k_2L_{1,N^{a-1}}^{a/a^{-1}} + (k_1 + k_2)L_{1,N^a}^{a/a^{-1}} \right) \right) - 2k_2L_{1,N^a}^{a/a^{-1}} - M \\
&= 1 - 2(M+1) \left(k_2L_{1,N^{a-1}}^{a/a^{-1}} + (k_1 + k_2)L_{1,N^a}^{a/a^{-1}} \right) - 2k_2L_{1,N^a}^{a/a^{-1}}.
\end{aligned} \tag{105}$$

Clearly, to satisfy stability we require that

$$2(M+1) \left(k_2 L_{1,N^{a-1}}^{a/a-1} + (k_1 + k_2) L_{1,N^a}^{a/a-1} \right) + 2k_2 L_{1,N^a}^{a/a-1} > 0. \quad (106)$$

Setting $k_1 > -4k_2$ and solving for $L_{1,N^{a-1}}^{a/a-1}/L_{1,N^a}^{a/a-1}$, we obtain the condition

$$\frac{L_{1,N^{a-1}}^{a/a-1}}{L_{1,N^a}^{a/a-1}} < 3 - \frac{1}{M+1}. \quad (107)$$

Invoking Proposition 2, statement (b.1), completes the proof. \square

In Figure 3 (a) the spectral radius of $\mathcal{P}^{p/p}$ is shown as a function of $k_2/k_1 \in (-0.25, 0.25]$ for an atomistic domain of size $M = 10$. We observe the expected behavior: if $k_1 + 4k_2$ is close to 0, $\sigma(\mathcal{P}^{p/p})$ is close to but strictly smaller than 1, and $\sigma(\mathcal{P}^{p/p}) \rightarrow 0$ as $k_2 \rightarrow 0$.

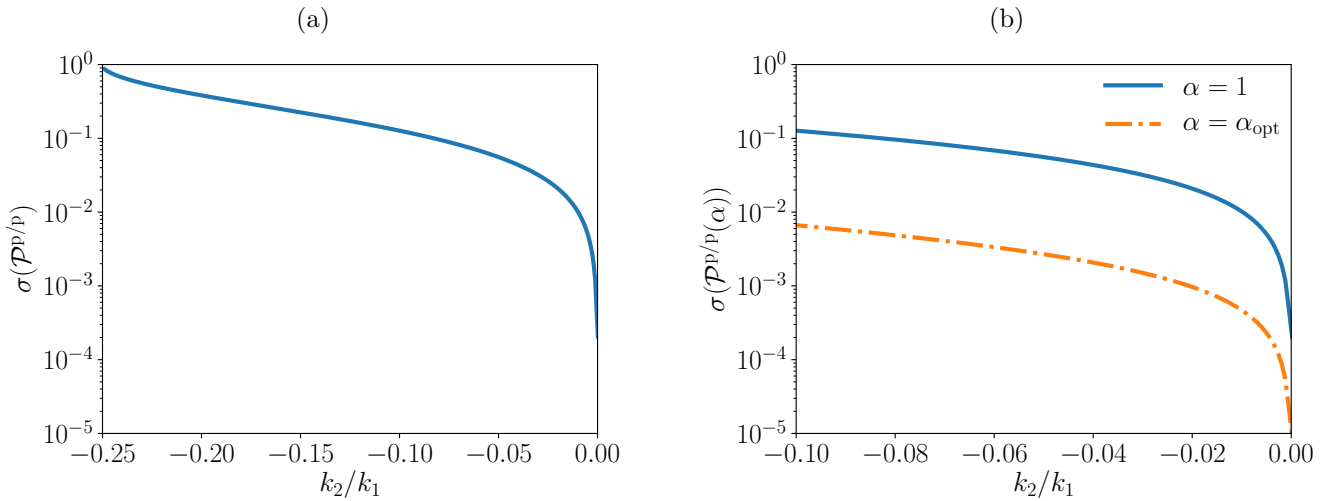


Figure 3: (a) Spectral radius of $\mathcal{P}^{p/p}$ as a function of the nonlocality ratio k_2/k_1 . (b) Spectral radius of $\mathcal{P}^{p/p}$ with and without optimal relaxation (Section 6.4)

6.4. Relaxation

Even though the convergence rate of the Sinclair method is far superior than the convergence rate of the alternating Schwarz method, it is not optimal. This is in particular crucial whenever \mathcal{L}_{hnl} and \mathcal{L}_{h} differ considerably. Although the solution in a region of interest in the atomistic domain may still be considered as good enough in such cases, intermediate solutions in the vicinity of the artificial interface will be non-smooth, slowing down the convergence.

One approach to accelerate the speed of convergence of domain decomposition solvers is relaxation (see, e.g., [33]). The underlying idea is to control the transmission conditions between both problems in an optimal way by augmenting the artificial boundary conditions with a relaxation parameter. Here, we will relax the magnitude of the inhomogeneous force f_{inh} . Therefore, we define the relaxation parameter $\alpha > 0$ and let

$$f_{\text{inh},k+1} = f_{\text{inh},k+1}(\alpha) = \alpha f_{\text{inh},k+1} \quad (108)$$

The solution in Λ^c in the $k+1$ -th iteration is now given by

$$u_{k+1}^c = u_{k+1}^c(\alpha) = u_k^c - \mathcal{S}^{c/c-1}[f_{\text{inh},k+1}(\alpha)] = \alpha u_{k+1}^c(\alpha = 0) + (1 - \alpha) u_k^c. \quad (109)$$

The anharmonic and the harmonic problem in each iteration are then defined as follows

$$(\mathbf{AH})_{k+1} \begin{cases} \mathcal{L}[\{u_{k+1}^a, u_{k+1}^p\}] = f_{\text{ext}} & \text{in } \Lambda^a, \\ u_{k+1} = u_k^c & \text{on } \Lambda^p, \end{cases} \quad (\mathbf{H})_{k+1} \begin{cases} \mathcal{L}_h[u_{h,k+1}] = \mathcal{L}_h^{a/a}[u_{h,0}] + \mathcal{L}_h^{a/c}[u_0] & \text{in } \Lambda^a, \\ \mathcal{L}_h[u_{h,k+1}] = -\mathcal{L}_h^{c/a}(\alpha)[u_{\text{ah},k+1}] + f_{\text{ext}} & \text{in } \Lambda^c, \\ u = \bar{u} & \text{on } \Lambda^I, \end{cases} \quad (110)$$

where

$$\mathcal{L}_h^{c/a}(\alpha)[u_{\text{ah},k+1}] = \alpha \sum_{i=1}^{k+1} f_{\text{inh},i}. \quad (111)$$

Analogously to Section 6.1, we can recast problem (110) into a projection method:

Lemma 2 (Projection operator for the relaxed Sinclair method). *Let u be a unique solution to (40). Then, problem (110) can be written as a projection method, that is,*

$$u_{k+1} - u = \mathcal{P}(\alpha)[u_k - u] \quad \text{in } \Lambda, \quad (112)$$

with the projection operator $\mathcal{P}(\alpha) : \mathcal{V} \rightarrow \mathcal{V}$ given by

$$\mathcal{P}(\alpha) = \begin{pmatrix} \mathcal{P}^{a/a} & \mathcal{P}^{a/c} \\ \mathcal{P}^{c/a} & \mathcal{P}^{c/c}(\alpha) \end{pmatrix} = \begin{pmatrix} \mathbf{0}^{a/a} & \mathcal{L}_{\text{hnl}}^{a/a-1} \mathcal{L}_{\text{hnl}}^{a/c} \\ \mathbf{0}^{c/a} & \mathcal{I}^{c/c} - \mathcal{S}^{c/c-1} (\mathcal{L}_h^{c/c}(\alpha) - \mathcal{L}_h^{c/a}(\alpha) \mathcal{L}_{\text{hnl}}^{a/a-1} \mathcal{L}_{\text{hnl}}^{a/c}) \end{pmatrix}. \quad (113)$$

Moreover, $\mathcal{P}^{a/c}$ is given by (56) and

$$\mathcal{P}^{c/c}(\alpha) = \begin{pmatrix} \mathcal{P}^{c/p}(\alpha) & \mathbf{0}^{c/c \setminus p} \end{pmatrix}, \quad \text{with } \mathcal{P}^{c/p}(\alpha) = \mathcal{P}_1^{c/p} + \alpha \mathcal{P}_2^{c/p} + (1 - \alpha) \mathcal{P}_3^{c/p}, \quad (114)$$

where $\mathcal{P}_1^{c/p}$ and $\mathcal{P}_2^{c/p}$ are given by (58) and

$$\mathcal{P}_3^{c/p} = (\mathcal{G}^{c/i+} - \mathcal{B}^{c/l} \mathcal{G}^{l/i+}) \mathcal{L}_h^{i+/p}. \quad (115)$$

Lemma 2 is a generalization of Lemma 1 since $\mathcal{P}(\alpha)$ reduces to \mathcal{P} as $\alpha \rightarrow 1$.

Sketch of the proof. We do not give a full proof for compactness as it would largely resemble the proof of Lemma 1. The essential idea is to write the α -dependent operators as

$$\mathcal{L}_h^{c/c}(\alpha) = \begin{pmatrix} \alpha \mathcal{L}_h^{i+/c} \\ \mathcal{L}_h^{c \setminus i+/c} \end{pmatrix}, \quad \mathcal{L}_h^{c/a}(\alpha) = \begin{pmatrix} \alpha \mathcal{L}_h^{i+/a} \\ \mathcal{L}_h^{c \setminus i+/a} \end{pmatrix}. \quad (116)$$

The next step is then to evaluate $\mathcal{G}^{c/c} \mathcal{L}_h^{c/c}(\alpha)$ which will be equivalent to $\mathcal{G}^{c/c} \mathcal{L}_h^{c/c}$ plus the remainder $\mathcal{G}^{c/i+} \mathcal{L}_h^{i+/c}$, where $\mathcal{G}^{c/i+} \mathcal{L}_h^{i+/p}$ is the finite boundary contribution occurring in $\mathcal{P}_3^{c/p}$. \square

From the structure of the projection operator \mathcal{P}_α it can be immediately deduced that Theorem 1 also holds for the relaxed Sinclair method. Thus, the *optimal relaxation factor* is the one which minimizes the spectral radius of $\mathcal{P}^{p/p}(\alpha)$

$$\alpha_{\text{opt}} := \arg \left\{ \min_{\alpha} \sigma(\mathcal{P}^{p/p}(\alpha)) \right\}. \quad (117)$$

In Figure 3 (b) it is shown that $\sigma(\mathcal{P}^{p/p}(\alpha_{\text{opt}}))$ is more than an order of magnitude smaller than $\sigma(\mathcal{P}^{p/p})$ in selected interval $k_2/k_1 \in [-0.1, 0]$.

7. Dynamic relaxation

For nonlinear problems, computing *the* optimal relaxation parameter in advance may not be the optimal choice since the atomistic operator \mathcal{L} potentially changes in every nonlinear iteration. It seems thus more practical to dynamically update α after *every* global iteration.

To compute an approximation of the optimal α , we choose to linearize the problem around $u_{k+1/2} = \{u_{k+1}^a, u_k^c\}$. Let u now be the solution to this linearized problem, it then follows from (54) that

$$u_{k+1} - u = \mathcal{P}(u_{k+1/2}; \alpha)[u_k - u]. \quad (118)$$

Equation (118) is still not practical since we do not want to solve the eigenvalue problem (117) in every iteration. Therefore, we convert (118) into a problem which minimizes the difference between two *iterates* by subtracting (118) from $u_{k+2} - u_k$ which yields

$$u_{k+2} - u_{k+1} = \mathcal{P}(u_{k+1/2}; \alpha)[u_{k+1} - u_k]. \quad (119)$$

The *optimal dynamic relaxation parameter* is then defined as the one which minimizes the maximum element of the projection (119) onto $\mathcal{V}(\Lambda^P)$, that is,

$$\alpha_{\text{opt}}^{\text{dyn}} := \arg \left\{ \min_{\alpha} \|\mathcal{P}^{\text{P/P}}(u_{k+1/2}; \alpha)[u_{k+1} - u_k]\|_{l^\infty} \right\}. \quad (120)$$

Evaluating $\alpha_{\text{opt}}^{\text{dyn}}$ yet requires the additional computation of a continuum and a linearized atomistic problem, which follows from the definition of $\mathcal{P}(u_{k+1/2}; \alpha)$ (cf., Lemma 2). Clearly, to be efficient, this method thus necessitates that the assumptions

- (i) solving **(H)** is significantly cheaper than solving **(AH)**,
- (ii) solving the linearized atomistic problem is significantly cheaper than solving the fully nonlinear problem **(AH)**,

hold, in which by “significantly cheaper” we roughly mean an order of magnitude. Assumption (i) has been verified in [12], where the elapsed time to solve **(H)** using an efficient \mathcal{H} -matrix solver [2] was found to be of the same order than a *single* evaluation of the atomistic force $\delta \Pi^a$. Assumption (ii) can be justified considering the solution of a nonlinear problem as a sequence of many linear problems. Moreover, when using a solver which builds Hessians (or approximations thereof), we can *reuse* $\mathcal{L}^{a/a}(u_{k+1/2})$ and $\mathcal{L}^{a/P}(u_{k+1/2})$. Since most of the time is usually spend on *building* $\mathcal{L}^{a/a}$ and $\mathcal{L}^{a/P}$, the time for solving the linear system is well-compensated. Furthermore, we can employ the solution to the linearized atomistic problem as an initial guess to the subsequent nonlinear iteration. In this respect, we can view the proposed relaxation method as a predictor-correcter scheme in which the linearized (trial) step is used to correct the boundary condition on **(AH)**_{k+2}.

Algorithm 3 shows the essential steps to compute $\alpha_{\text{opt}}^{\text{dyn}}$. This algorithm can be directly integrated into Algorithm 2 before line 13. In the results section, we refer to the Sinclair method with dynamic relaxation as **SincDynRelax**.

Algorithm 3: Dynamic relaxation (DynRelax)

Input: optimal relaxation parameter $\alpha_{\text{opt},k}^{\text{dyn}}$ and solution $u_{k+1/2}$ from previous iteration,
inhomogeneous force $f_{\text{inh},k+1}$; natural boundary condition u^{I}

- 1 $f_{\text{inh},k+1} \leftarrow \alpha_{\text{opt},k}^{\text{dyn}} f_{\text{inh},k+1}, \quad \tilde{u}_{k+1}^{\text{I}} \leftarrow -\mathcal{G}^{\text{I/I}^+}[f_{\text{inh},k+1}^{\text{I}^+}]; \quad // \text{ relax inhomogeneous force}$
- 2 $u_{\text{trial},k+1}^{\text{P}} \leftarrow u_k^{\text{P}} + \text{DBEM}(\tilde{u}^{\text{I}} - u_k^{\text{I}}, -f_{\text{inh}}); \quad // \text{ compute trial solution}$
- 3 $w_1 \leftarrow \mathcal{P}_1^{\text{P/P}}[u_{\text{trial},k+1} - u_k], \quad w_3 \leftarrow \mathcal{P}_3^{\text{P/P}}[u_{\text{trial},k+1} - u_k],$
 $w_2 \leftarrow \mathcal{P}_2^{\text{P/P}}(u_{k+1/2})[u_{\text{trial},k+1} - u_k]; \quad // \text{ compute the projections}$
- 4 $\alpha_{\text{opt},k+1}^{\text{dyn}} \leftarrow \arg \left\{ \min_{\alpha} \|(w_1 + w_3) + \alpha(w_2 - w_3)\|_{l^\infty} \right\}; \quad // \text{ update } \alpha$

Output: optimal dynamic relaxation parameter $\alpha_{\text{opt},k+1}^{\text{dyn}}$

Remark 4. *The dynamic relaxation method is optimal in the following sense*

$$\begin{aligned} \|u_{k+2}^{\text{P}} - u_{k+1}^{\text{P}}\|_{l^\infty} = \|\mathcal{P}^{\text{P/P}}(u_{k+1/2}; \alpha_{\text{opt}}^{\text{dyn}})[u_{k+1} - u_k]\|_{l^\infty} &\leq \|\mathcal{P}^{\text{P/P}}(u_{k+1/2}; \alpha_{\text{opt}}^{\text{dyn}})[u_{k+1} - u_k]\| \\ &\stackrel{(117)}{\leq} \|\mathcal{P}^{\text{P/P}}(u_{k+1/2}; \alpha_{\text{opt}})[u_{k+1} - u_k]\| \\ &\leq \|\mathcal{P}^{\text{P/P}}(u_{k+1/2}; \alpha_{\text{opt}})\| \|u_{k+1}^{\text{P}} - u_k^{\text{P}}\| \\ &\lesssim \sigma(\mathcal{P}^{\text{P/P}}(u_{k+1/2}; \alpha_{\text{opt}})) \|u_{k+1}^{\text{P}} - u_k^{\text{P}}\|. \end{aligned} \quad (121)$$

8. Numerical examples

In this section, we present some selected numerical experiments for linear and nonlinear problems. Thereby, we focus solely on the convergence properties of the Sinclair method since detailed error analyses of force-based A/C coupling methods have already been extensively discussed elsewhere (e.g., [22, 17]).

8.1. Linear problem

We first consider a linear problem. This problem mainly serves for testing purposes to validate the bound (80). We set the size of the entire and the atomistic domain to $N = 100$ and $M = 10$, respectively. Further, we apply a point force at $\xi/a_0 = 5$ in the atomistic domain, which is slightly off-center to rule out symmetry effects. We then set the boundary condition according to the values of the analytic Green function (26), i.e.,

$$u(\xi/a_0 = -N - 1) = G(\xi/a_0 = -N - 1), \quad u(\xi/a_0 = N + 1) = G(\xi/a_0 = N + 1). \quad (122)$$

The atomistic model is assumed to comprise second nearest neighbor interactions such that the force constant tensor is given by (91).

In the following we therefore investigate the behavior for various ratios k_2/k_1 . Depending on this ratio the gradient of the solution $\nabla u(\xi)$ has a different behavior in the atomistic domain. Exemplary results are presented in Figure 4 which show a rather sharp gradient for $k_2/k_1 = -1/50$ and a significantly wider and smoother transition region for $k_2/k_1 = -1/5$.

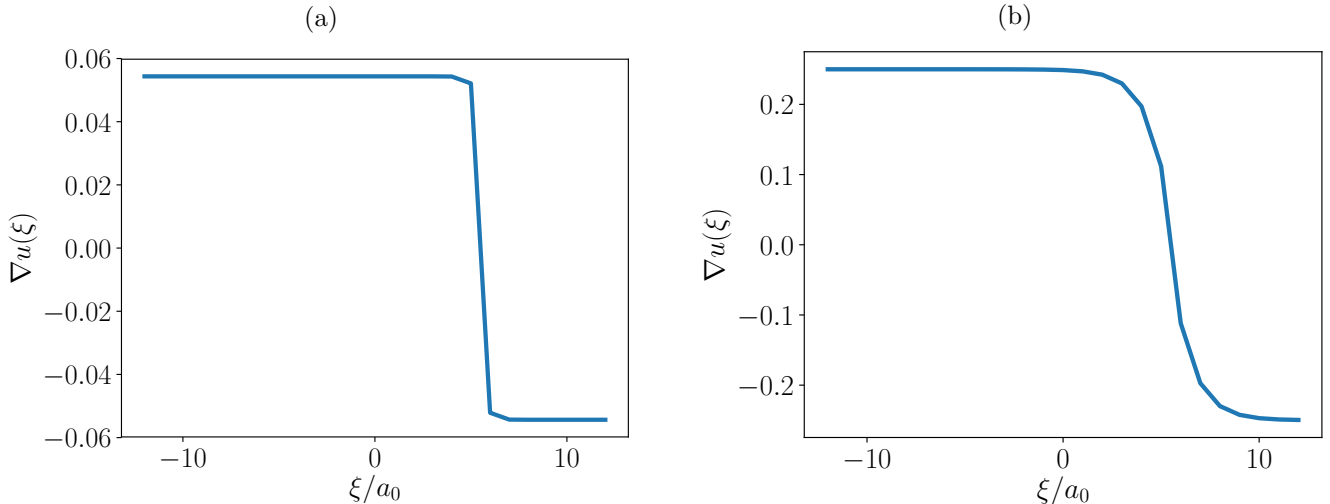


Figure 4: Gradient of the solution for the linear problem from Section 8.1; (a) $k_2/k_1 = -1/50$, (b) $k_2/k_1 = -1/5$

Table 1 shows the relative errors of the A/C coupling with respect to the fully atomistic reference solution u_{ref} in the l^2 - and energy norms

$$\epsilon = \frac{\|u_{\text{ref}} - u\|}{\|u_{\text{ref}}\|}, \quad \epsilon_{\nabla} = \frac{\|\nabla u_{\text{ref}} - \nabla u\|}{\|\nabla u_{\text{ref}}\|}. \quad (123)$$

The values are reasonable, given the fact the gradient is close to a constant in the vicinity of the artificial interface (cf., Figure 4, where $A^i := \{-10, 10\}$). In addition, the total number of iterations N_{iter} and $N_{\text{iter}}^{\text{relax}}$ corresponding to **Sinc** and **SincRelax**, respectively, are shown, in addition to their convergence rates σ and σ_{opt} from Figure 3. The results are expected in the sense that the number of required iterations increases as k_2/k_1 decreases. In both cases a relaxation of

k_2/k_1	ϵ	ϵ_{∇}	N_{iter}	σ	$N_{\text{iter}}^{\text{relax}}$	σ_{opt}
-1/50	1.1e-10	7.3e-10	7	0.021	5	0.00097
-1/5	0.00303	0.00309	24	0.38	8	0.029

Table 1: Global error, number of iterations and convergence rates of **Sinc** and **SincRelax** for various ratios k_2/k_1

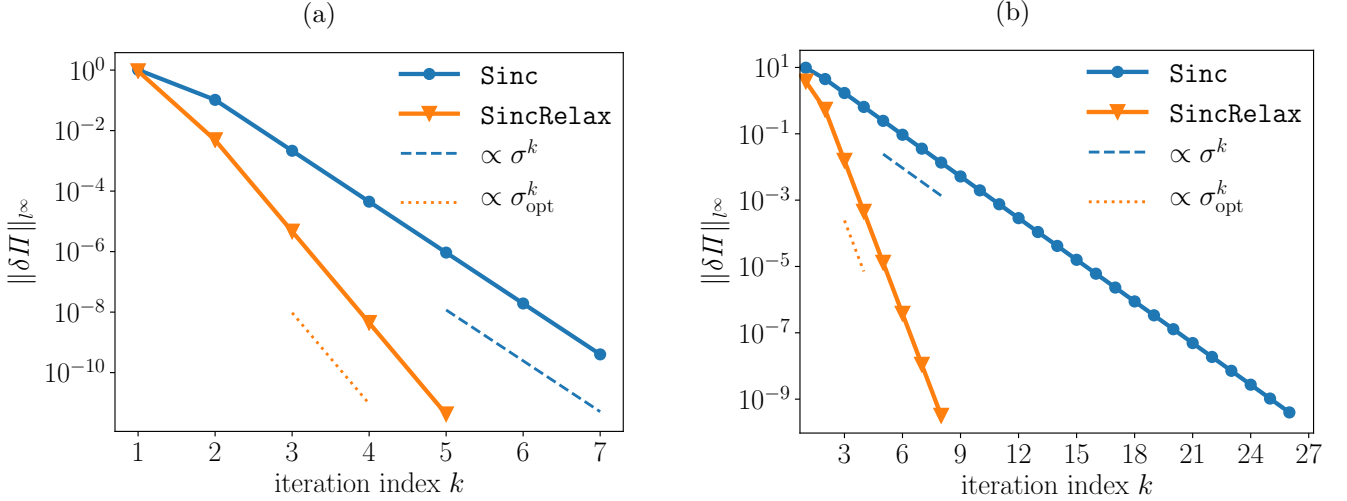


Figure 5: Displacement increment and bound as a function of the iteration index k for the Sinclair method with and without relaxation; (a) $k_2/k_1 = -1/50$, (b) $k_2/k_1 = -1/5$

the inhomogeneous force improves the speed of convergence by a factor of ≈ 1.5 -3. Moreover, from Figure 5 we observe that the computed bounds are sharp.

8.2. Nonlinear problem

We now turn to a nonlinear problem. For this class of test problems we select the Morse potential [20] which has already previously been employed to validate related A/C coupling methods (e.g., [35, 12]). The corresponding site energy is given by

$$\mathcal{E}_\xi(u(\eta) - u(\xi)) = \sum_{\eta \in \mathcal{R}_\xi} D e^{-2a(r(u(\eta) - u(\xi)) - r_0)} - 2D e^{-a(r(u(\eta) - u(\xi)) - r_0)}. \quad (124)$$

The parameters of the Morse potential are chosen in such a way to mimic those of aluminum [8], i.e.,

$$D_0 = 0.2703 \text{ eV}, \quad a = 1.1646 \text{ \AA}, \quad r_0 = 3.253 \text{ \AA}. \quad (125)$$

We assume second nearest-neighbor interactions which yields the equilibrium lattice constant $a_0 = 3.214 \text{ \AA}$. The force constants corresponding to this atomistic model are

$$k_1 = 0.838 \text{ eV/\AA}^2, \quad k_2 = -0.0173 \text{ eV/\AA}^2, \quad k_2/k_1 \approx -1/50 \quad (126)$$

and, therefore, $\bar{k} = 0.769 \text{ eV/\AA}^2$.

In order to construct the reference problem, we impose the displacement

$$u_{\text{ref}}(\xi) = 0.23 \cdot \xi(1 + (\xi/a_0 - 5)^2)^{-\beta/2}, \quad (127)$$

where the parameter β allows us to tune the far-field behavior of the solution corresponding to more realistic scenarios in two and three dimensions. That is, $\beta < 1$ implies a divergent behavior of the solution, corresponding to straight dislocations and cracks. Vice versa, $\beta > 1$ implies a decaying solution, corresponding to vacancies, interstitials or dislocation loops. Here, we present numerical examples for $\beta = 0.8$ (diverging solution) and $\beta = 1.5$ (decaying solution), shown in Figure 6 and Figure 7. Given u_{ref} , we compute the right hand side as follows

$$\forall \xi \in \Lambda \quad f_{\text{ext}}(\xi) = \mathcal{L}[u_{\text{ref}}](\xi) \quad (128)$$

and subsequently apply it to the coupled problem. Since the solution of the global harmonic problem $u_{\text{h}}^{\text{glo}}$ differs considerably from the fully atomistic solution we have set $u_0 = 0$.

In order to solve the nonlinear atomistic problem **(AH)**, we employ a standard Newton scheme with a conjugate gradient method to solve the linear system in each iteration. To assess the quality of the dynamic relaxation method, we define N_{H^a} , $N_{\delta H^a}$ and $N_{\delta^2 H^a}$ as the number of atomistic energy, force and hessian evaluations, and, additionally, N_{iter} and Δt as the number of global iterations and the elapsed time for running a basic Python implementation of the

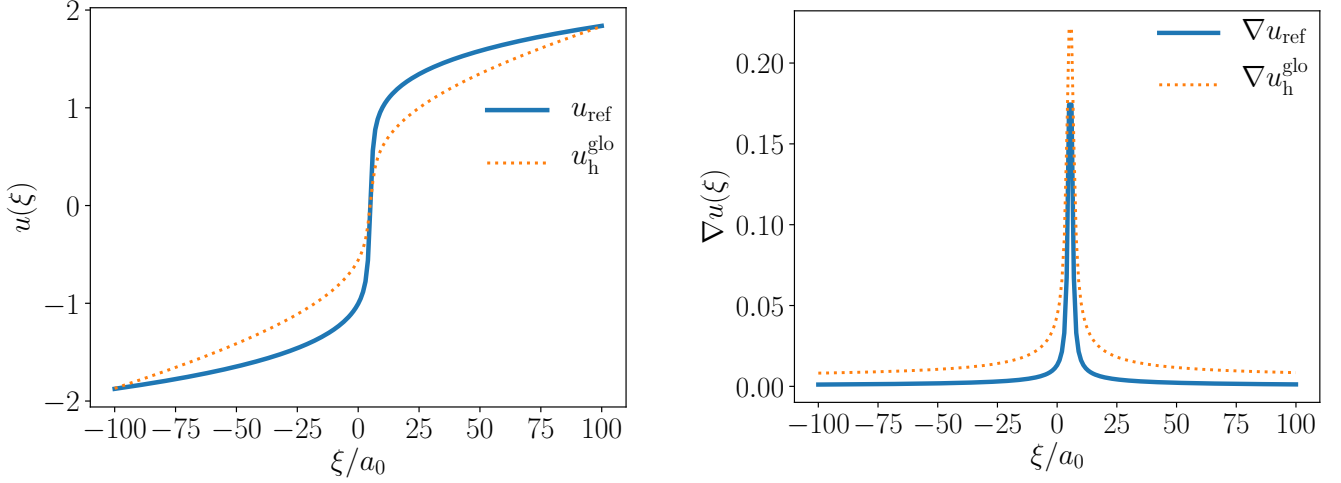


Figure 6: Diverging solution ($\beta = 0.8$) and its gradient

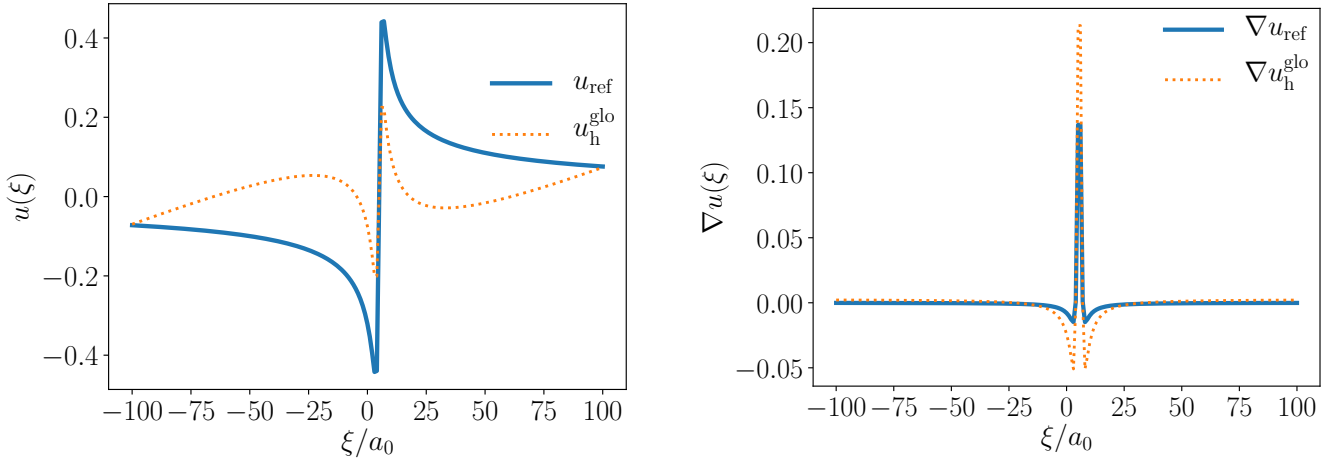


Figure 7: Decaying solution ($\beta = 1.5$) and its gradient

domain decomposition algorithm. The same quantities with superscript relax, i.e., \bullet^{relax} , refer to the Sinclair method with dynamic relaxation.

The results for $M = 15, 25, 35$ are presented in Table 2 and 3. It can be seen that the speed of convergence is slower, when compared to the linear case, although the atomistic problem is rather localized and the error is acceptable. While the standard Sinclair method is still very fast in comparison with related staggered solvers (e.g., [22]), dynamic relaxation leads to an additional speedup. This behavior is exemplified in Figure 8 for $M = 25$, showing a decay which is close to the optimal (static) convergence rate σ_{opt} after a few iterations.

M	ϵ	ϵ_{∇}	N_{Π^a}	$N_{\delta\Pi^a}$	$N_{\delta^2\Pi^a}$	N_{iter}	Δt [s]	$N_{\Pi^a}^{\text{relax}}$	$N_{\delta\Pi^a}^{\text{relax}}$	$N_{\delta^2\Pi^a}^{\text{relax}}$	$N_{\text{iter}}^{\text{relax}}$	Δt^{relax} [s]
15	0.035	0.049	78	75	59	19	0.35	50	37	32	7	0.18
25	0.0098	0.017	72	67	56	16	0.48	36	34	30	6	0.23
35	0.0046	0.0081	63	61	50	13	0.63	50	33	31	6	0.37

Table 2: Global error, number of function evaluations and elapsed time for different sizes of the atomistic domain M with and without dynamic relaxation for the diverging solution ($\beta = 0.8$)

M	ϵ	ϵ_{∇}	N_{Π^a}	$N_{\delta\Pi^a}$	$N_{\delta^2\Pi^a}$	N_{iter}	Δt [s]	$N_{\Pi^a}^{\text{relax}}$	$N_{\delta\Pi^a}^{\text{relax}}$	$N_{\delta^2\Pi^a}^{\text{relax}}$	$N_{\text{iter}}^{\text{relax}}$	Δt^{relax} [s]
15	0.18	0.016	47	45	36	11	0.19	28	28	22	6	0.12
25	0.031	0.0033	37	35	29	8	0.25	26	23	21	5	0.17
35	0.011	0.0012	33	31	26	7	0.36	22	21	18	4	0.21

Table 3: Global error, number of function evaluations and elapsed time for different sizes of the atomistic domain M with and without dynamic relaxation for the decaying solution ($\beta = 1.5$)

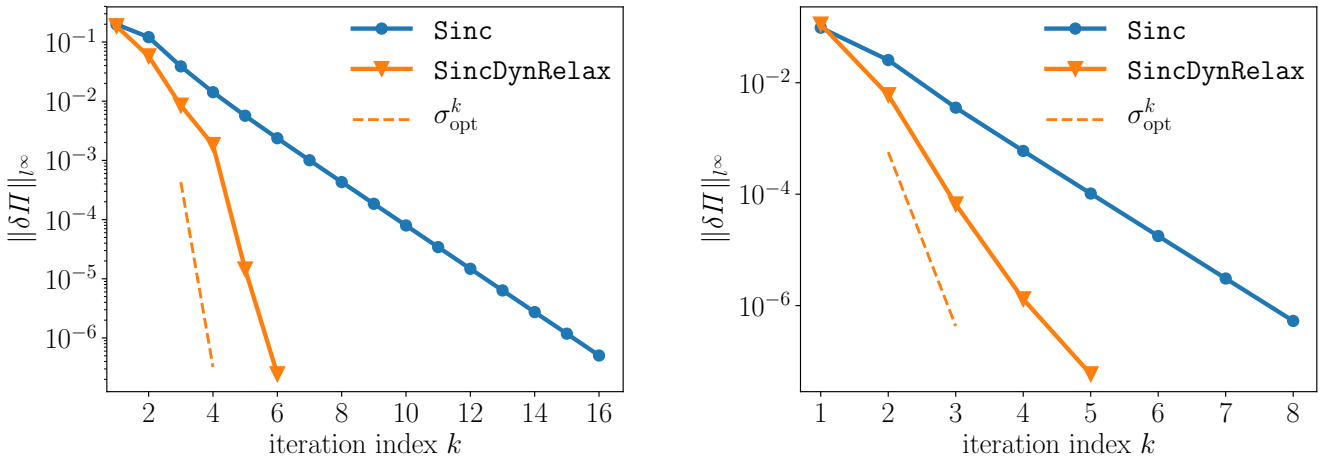


Figure 8: Displacement increment as a function of the iteration for $M = 25$; left: diverging solution ($\beta = 0.8$), right: decaying solution ($\beta = 1.5$)

9. Conclusions

We have developed and analyzed a new domain decomposition solver for force-based atomistic/continuum coupling. The proposed solver extends the method of Sinclair [30], developed in the 1970s for effectively infinite problems, to bounded domains. The novelty of the proposed method is the splitting of the global differential operator into a finite anharmonic and an infinite harmonic part which stands in contrast to existing methods which partition the problem into separated domains. We have analyzed the method under homogeneous loading conditions and shown that this splitting gives rise to significantly improved convergence rates over classical methods (e.g., alternating Schwarz). Furthermore, a dynamic relaxation method for general nonlinear problems has been proposed further reducing the number of necessary iterations by a factor of 1.5–2.5.

We have also incorporated several practical aspects in our analysis. First, we have used a discrete boundary element method in order to solve the global harmonic problem and, therefore, an explicit discretization of the interior domain is not required. In a previous publication [12], we have shown that this method can be efficiently combined with hierarchical approximations of the dense system matrices, reducing the computational complexity to $\#DOF \log(\#DOF)$ and allowing for large-scale simulations with possibly hundreds of thousands of real atoms. Second, we have shown that the harmonic problem does not require a priori knowledge of the exact behavior in the atomistic domain. Although an initial guess can improve the pre-asymptotic convergence behavior, it is not crucial. Third, we generally remark that domain decomposition solvers share the attractive advantage to be easily integrable into existing molecular dynamics codes which is a crucial requirement for practical application.

While the proposed method is general, we have not discussed various other points which require additional attention:

- Stability analysis in two and three dimensions.
- Efficiency of the dynamic relaxation method in two and three dimensions and application of other acceleration techniques (e.g., overlapping subdomains).
- Adequacy of the method to be used as a preconditioner for monolithic Krylov subspace solvers.

Currently we are working on an efficient three-dimensional implementation including an approximation of the solution on the outer boundary (see Remark 2) in combination with an \mathcal{H} -matrix solver. Results will be reported in a future article.

For our proof we further require an upper bound for the diagonal elements of \underline{U} . For this purpose we compute the first three components

$$U_{1,1} = -1, \quad U_{2,2} = -2kk_2 - 1, \quad U_{3,3} = \frac{4kk_2 + k_2^2 + 1}{-2kk_2 - 1}. \quad (\text{A.5})$$

Subsequently, using (A.4), we can write

$$\forall i = 4, \dots, K \quad U_{i,i} = -1 + \frac{2kk_2}{U_{i-1,i-1}} - \frac{k_2^2}{U_{i-1,i-1}U_{i-2,i-2}} - 1 \frac{k_2^4}{U_{i-1,i-1}U_{i-2,i-2}U_{i-3,i-3}}. \quad (\text{A.6})$$

From (A.5) we deduce that for $k_2 \geq k_2^*$ and $i = 1, 2, 3$, $U_{i,i}(k_2) \leq U_{i,i}(k_2^*)$. To generalize this result, we explicitly compute the diagonal components $\bar{U}_{i,i} = U_{i,i}(-1/4)$ for the limiting case when $k_2 = -1/4$, that is,

$$\bar{U}_{1,1} = \frac{4}{4}, \quad \bar{U}_{2,2} = \frac{5}{8}, \quad \bar{U}_{3,3} = \frac{6}{12}, \quad \bar{U}_{4,4} = \frac{7}{16}, \quad \bar{U}_{5,5} = \frac{8}{20}, \quad \dots, \quad \bar{U}_{K,K} = -(1 + 3K^{-1})/4, \quad (\text{A.7})$$

where last expression can be readily checked by using $U_{K-1,K-1} = -(1+3(K-1)^{-1})/4$, $U_{K-2,K-2} = -(1+3(K-2)^{-1})/4$ and $U_{K-3,K-3} = -(1+3(K-3)^{-1})/4$ in (A.6).

It follows that $\bar{U}_{K,K}$ is bounded by $\{-1, -1/4\}$. Using (A.5), it can then be shown inductively, e.g., by employing a straightforward contradiction argument, that

$$\forall K > 1 \quad U_{K,K} < -(1 + 3K^{-1})/4. \quad (\text{A.8})$$

Appendix A.2. Proof of statement (a)

Using the representation (A.1), the inverse coefficients read

$$L_{1,1}^{a/a-1} = \frac{C_{1,1}}{\det(\underline{L}^{a/a})}, \quad L_{1,N^a}^{a/a-1} = \frac{C_{1,N^a}}{\det(\underline{L}^{a/a})}. \quad (\text{A.9})$$

Since $\underline{L}^{a/a}$ is positive definite it follows that $\det(\underline{L}^{a/a}) > 0$. Therefore, it remains to check that both numerators are positive. For $C_{1,1}$ this is trivially true since positive definiteness of $\underline{L}^{a/a}$ holds independently of its size. For the second term we find that

$$C_{1,N^a} = (-1)^{1+N^a} \det(\underline{M}_{N^a,1}) = \det(\underline{M}_{N^a,1}) = \det(\underline{LU}) = \det(\underline{U}) > 0, \quad (\text{A.10})$$

where the latter inequality follows from the fact $\underline{U} \in \mathbb{R}^{K \times K}$ and that $\forall i = 1, \dots, K$ $U_{i,i} < 0$. \square

Appendix A.3. Proof of statement (b)

To prove the second statement, we introduce the shift matrix $\underline{J} = \underline{M}_{N^a,1}^{-1} \underline{M}_{N^a-1,1}$ to obtain

$$\frac{L_{1,N^a-1}^{a/a-1}}{L_{1,N^a}^{a/a-1}} = -\frac{\det(\underline{M}_{N^a-1,1})}{\det(\underline{M}_{N^a,1})} = -\frac{\det(\underline{M}_{N^a,1} \underline{J})}{\det(\underline{M}_{N^a,1})} = -\det(\underline{J}). \quad (\text{A.11})$$

The matrix \underline{J} is the upper triangular matrix

$$\underline{J} = \begin{pmatrix} \underline{I} & \underline{v} \\ \underline{0}^\top & \det(\underline{J}) \end{pmatrix}. \quad (\text{A.12})$$

Again, using the factorized representation of $\underline{M}_{N^a,1}$ the determinant of \underline{J} follows as

$$\det(\underline{J}) = -\frac{2k}{U_{K,K}} + \frac{k_2}{U_{K,K}U_{K-1,K-1}} + \frac{k_2^3}{U_{K,K}U_{K-1,K-1}U_{K-2,K-2}}. \quad (\text{A.13})$$

Combining (A.13) and (A.8) in (A.11) we obtain the result stated in (b.1).

Statement (b.2) is a corollary of statement (b.1). To prove it, we use the fact that $\det(\underline{M}_{1,1})$ can be represented as

$$\det(\underline{M}_{1,1}) = \det(\underline{M}_{1,N^a}) + \det(\underline{A}), \quad (\text{A.14})$$

with

$$\underline{A} = \underline{M}_{1,1} + \underline{v}\underline{w}^T, \quad \text{with } \underline{v} = (0, \dots, 0, 1)^T, \quad \underline{w} = (1, k_2, 0, \dots, 0)^T, \quad (\text{A.15})$$

which can be derived using the properties of determinants. Using the matrix determinant lemma, we can write

$$\begin{aligned} \det(\underline{A}) &= (1 + \underline{w}^T \underline{M}_{1,1}^{-1} \underline{v}) \det(\underline{M}_{1,1}) \\ &= \left(1 + (\underline{M}_{1,1}^{-1})_{1,K} + k_2 (\underline{M}_{1,1}^{-1})_{1,K-1}\right) \det(\underline{M}_{1,1}) \\ &> \left(1 - 4k_2 (\underline{M}_{1,1}^{-1})_{1,K} + k_2 (\underline{M}_{1,1}^{-1})_{1,K-1}\right) \det(\underline{M}_{1,1}) \\ &> 0 \end{aligned} \quad (\text{A.16})$$

where the last inequality follows immediately from statement (b.1). Thus, we have

$$\frac{L_{1,1}^{a/a-1}}{L_{1,N^a}^{a/a-1}} = \frac{\det(\underline{M}_{1,1})}{\det(\underline{M}_{N^a,1})} = \frac{\det(\underline{M}_{N^a,1}) + \det(\underline{A})}{\det(\underline{M}_{N^a,1})} > 1. \quad (\text{A.17})$$

□

References

- [1] Argon, A., Aug. 2007. Strengthening Mechanisms in Crystal Plasticity. Oxford University Press.
URL <http://www.oxfordscholarship.com/view/10.1093/acprof:oso/9780198516002.001.0001/acprof-9780198516002>
- [2] Bebendorf, M., 2008. Hierarchical matrices: a means to efficiently solve elliptic boundary value problems. No. 63 in Lecture notes in computational science and engineering. Springer, Berlin, oCLC: ocn220011087.
- [3] Cantoni, A., Butler, P., 1976. Eigenvalues and Eigenvectors of Symmetric Centrosymmetric Matrices. Linear Algebra and its Applications 13, 275–288.
- [4] Curtin, W. A., Miller, R. E., 2003. Atomistic/continuum coupling in computational materials science. Modelling and Simulation in Materials Science and Engineering 11 (3), 33–68.
URL <https://doi.org/10.1088/2F0965-0393/2F11/2F3/2F201>
- [5] Dobson, M., Luskin, M., Ortner, C., Jul. 2010. Stability, Instability, and Error of the Force-based Quasicontinuum Approximation. Archive for Rational Mechanics and Analysis 197 (1), 179–202, arXiv: 0903.0610.
URL <http://arxiv.org/abs/0903.0610>
- [6] Dobson, M., Luskin, M., Ortner, C., Sep. 2011. Iterative methods for the force-based quasicontinuum approximation: Analysis of a 1d model problem. Computer Methods in Applied Mechanics and Engineering 200 (37-40), 2697–2709.
URL <https://linkinghub.elsevier.com/retrieve/pii/S0045782510002203>
- [7] Fellingner, M. R., Tan, A. M. Z., Hector, L. G., Trinkle, D. R., Nov. 2018. Geometries of edge and mixed dislocations in bcc Fe from first-principles calculations. Physical Review Materials 2 (11).
URL <https://link.aps.org/doi/10.1103/PhysRevMaterials.2.113605>
- [8] Girifalco, L. A., Weizer, V. G., May 1959. Application of the Morse Potential Function to Cubic Metals. Physical Review 114 (3), 687–690.
URL <https://link.aps.org/doi/10.1103/PhysRev.114.687>
- [9] Greengard, L., Rokhlin, V., 1987. A Fast Algorithm for Particle Simulations. Journal of Computational Physics 73, 325–348.
- [10] Hackbusch, W., 1999. A Sparse Matrix Arithmetic based on H-Matrices. Part I: Introduction to H-Matrices. Computing 62, 89–108.
- [11] Hodapp, M., 2018. On flexible Green function methods for atomistic/continuum coupling. PhD thesis, École polytechnique fédérale de Lausanne.
- [12] Hodapp, M., Anciaux, G., Curtin, W., May 2019. Lattice Green function methods for atomistic/continuum coupling: Theory and data-sparse implementation. Computer Methods in Applied Mechanics and Engineering 348, 1039–1075.
URL <https://linkinghub.elsevier.com/retrieve/pii/S0045782519300775>
- [13] Kochmann, D. M., Venturini, G. N., Apr. 2014. A meshless quasicontinuum method based on local maximum-entropy interpolation. Modelling and Simulation in Materials Science and Engineering 22 (3), 034007.
URL <http://stacks.iop.org/0965-0393/22/i=3/a=034007?key=crossref.1c71666a6a31fc5b99b546047cf19d95>
- [14] Kohlhoff, S., Schmauder, S., 1989. A New Method for Coupled Elastic-Atomistic Modelling. In: Atomistic Simulation of Materials. Springer US, Boston, MA, pp. 411–418.
- [15] Li, X., Sep. 2009. Efficient boundary conditions for molecular statics models of solids. Physical Review B 80 (10), 104112.
URL <https://link.aps.org/doi/10.1103/PhysRevB.80.104112>
- [16] Li, X., Jun. 2012. An atomistic-based boundary element method for the reduction of molecular statics models. Computer Methods in Applied Mechanics and Engineering 225-228, 1–13.
URL <https://linkinghub.elsevier.com/retrieve/pii/S0045782512000825>
- [17] Luskin, M., Ortner, C., May 2013. Atomistic-to-continuum coupling. Acta Numerica 22, 397–508.
URL https://www.cambridge.org/core/product/identifier/S0962492913000068/type/journal_article
- [18] Martinsson, P.-G., 2002. Fast multiscale methods for lattice equations. PhD thesis, The University of Texas at Austin.
- [19] Martinsson, P.-G., Rodin, G. J., Aug. 2009. Boundary algebraic equations for lattice problems. Proceedings of the Royal Society A: Mathematical, Physical and Engineering Sciences 465 (2108), 2489–2503.
URL <http://www.royalsocietypublishing.org/doi/10.1098/rspa.2008.0473>

- [20] Morse, P. M., Jul. 1929. Diatomic Molecules According to the Wave Mechanics. II. Vibrational Levels. *Physical Review* 34 (1), 57–64.
URL <https://link.aps.org/doi/10.1103/PhysRev.34.57>
- [21] Ortner, C., Zhang, L., Sep. 2014. Energy-based atomistic-to-continuum coupling without ghost forces. *Computer Methods in Applied Mechanics and Engineering* 279, 29–45.
URL <https://linkinghub.elsevier.com/retrieve/pii/S0045782514002059>
- [22] Parks, M. L., Bochev, P. B., Lehoucq, R. B., Jan. 2008. Connecting Atomistic-to-Continuum Coupling and Domain Decomposition. *Multiscale Modeling & Simulation* 7 (1), 362–380.
URL <http://epubs.siam.org/doi/10.1137/070682848>
- [23] Pavia, F., Curtin, W. A., Jul. 2015. Parallel algorithm for multiscale atomistic/continuum simulations using LAMMPS. *Modelling and Simulation in Materials Science and Engineering* 23 (5), 055002.
URL <http://stacks.iop.org/0965-0393/23/i=5/a=055002?key=crossref.02ff7625c3b88ed47b97e830253f79d1>
- [24] Quarteroni, A., Sacco, R., Saleri, F., 2007. Numerical mathematics, 2nd Edition. No. 37 in Texts in applied mathematics. Springer, Berlin ; New York.
- [25] Rao, S., Hernandez, C., Simmons, J. P., Parthasarathy, T. A., Woodward, C., Jan. 1998. Green’s function boundary conditions in two-dimensional and three-dimensional atomistic simulations of dislocations. *Philosophical Magazine A* 77 (1), 231–256.
URL <http://www.tandfonline.com/doi/abs/10.1080/01418619808214240>
- [26] Shilkrot, L., Miller, R. E., Curtin, W. A., Apr. 2004. Multiscale plasticity modeling: coupled atomistics and discrete dislocation mechanics. *Journal of the Mechanics and Physics of Solids* 52 (4), 755–787.
URL <https://linkinghub.elsevier.com/retrieve/pii/S0022509603001625>
- [27] Shimokawa, T., Mortensen, J. J., Schiøtz, J., Jacobsen, K. W., Jun. 2004. Matching conditions in the quasicontinuum method: Removal of the error introduced at the interface between the coarse-grained and fully atomistic region. *Physical Review B* 69 (21), 214104.
URL <https://link.aps.org/doi/10.1103/PhysRevB.69.214104>
- [28] Sinclair, J. E., Dec. 1971. Improved Atomistic Model of a bcc Dislocation Core. *Journal of Applied Physics* 42 (13), 5321–5329.
URL <http://aip.scitation.org/doi/10.1063/1.1659943>
- [29] Sinclair, J. E., Mar. 1975. The influence of the interatomic force law and of kinks on the propagation of brittle cracks. *Philosophical Magazine* 31 (3), 647–671.
URL <http://www.tandfonline.com/doi/abs/10.1080/14786437508226544>
- [30] Sinclair, J. E., Gehlen, P. C., Hoagland, R. G., Hirth, J. P., Jul. 1978. Flexible boundary conditions and nonlinear geometric effects in atomic dislocation modeling. *Journal of Applied Physics* 49 (7), 3890–3897.
URL <http://aip.scitation.org/doi/10.1063/1.325395>
- [31] Tadmor, E. B., Ortiz, M., Phillips, R., Jun. 1996. Quasicontinuum analysis of defects in solids. *Philosophical Magazine A* 73 (6), 1529–1563.
URL <http://www.tandfonline.com/doi/abs/10.1080/01418619608243000>
- [32] Thomson, R., Zhou, S. J., Carlsson, A. E., Tewary, V. K., Nov. 1992. Lattice imperfections studied by use of lattice Green’s functions. *Physical Review B* 46 (17), 10613–10622.
URL <https://link.aps.org/doi/10.1103/PhysRevB.46.10613>
- [33] Toselli, A., Widlund, O. B., 2005. Domain decomposition methods—algorithms and theory. No. 34 in Springer series in computational mathematics. Springer, Berlin, oCLC: ocm56879011.
- [34] Tyrtshnikov, E., Jun. 1996. Mosaic-Skeleton approximations. *Calcolo* 33 (1-2), 47–57.
URL <http://link.springer.com/10.1007/BF02575706>
- [35] Van Koten, B., Li, X. H., Luskin, M., Ortner, C., 2012. A Computational and Theoretical Investigation of the Accuracy of Quasicontinuum Methods. In: Graham, I. G., Hou, T. Y., Lakkis, O., Scheichl, R. (Eds.), *Numerical Analysis of Multiscale Problems*. Vol. 83. Springer Berlin Heidelberg, Berlin, Heidelberg, pp. 67–96.
URL http://link.springer.com/10.1007/978-3-642-22061-6_3
- [36] Woodward, C., Rao, S. I., May 2002. Flexible *Ab Initio* Boundary Conditions: Simulating Isolated Dislocations in bcc Mo and Ta. *Physical Review Letters* 88 (21).
URL <https://link.aps.org/doi/10.1103/PhysRevLett.88.216402>
- [37] Zhang, F. (Ed.), 2005. The Schur complement and its applications. No. v. 4 in Numerical methods and algorithms. Springer, New York.